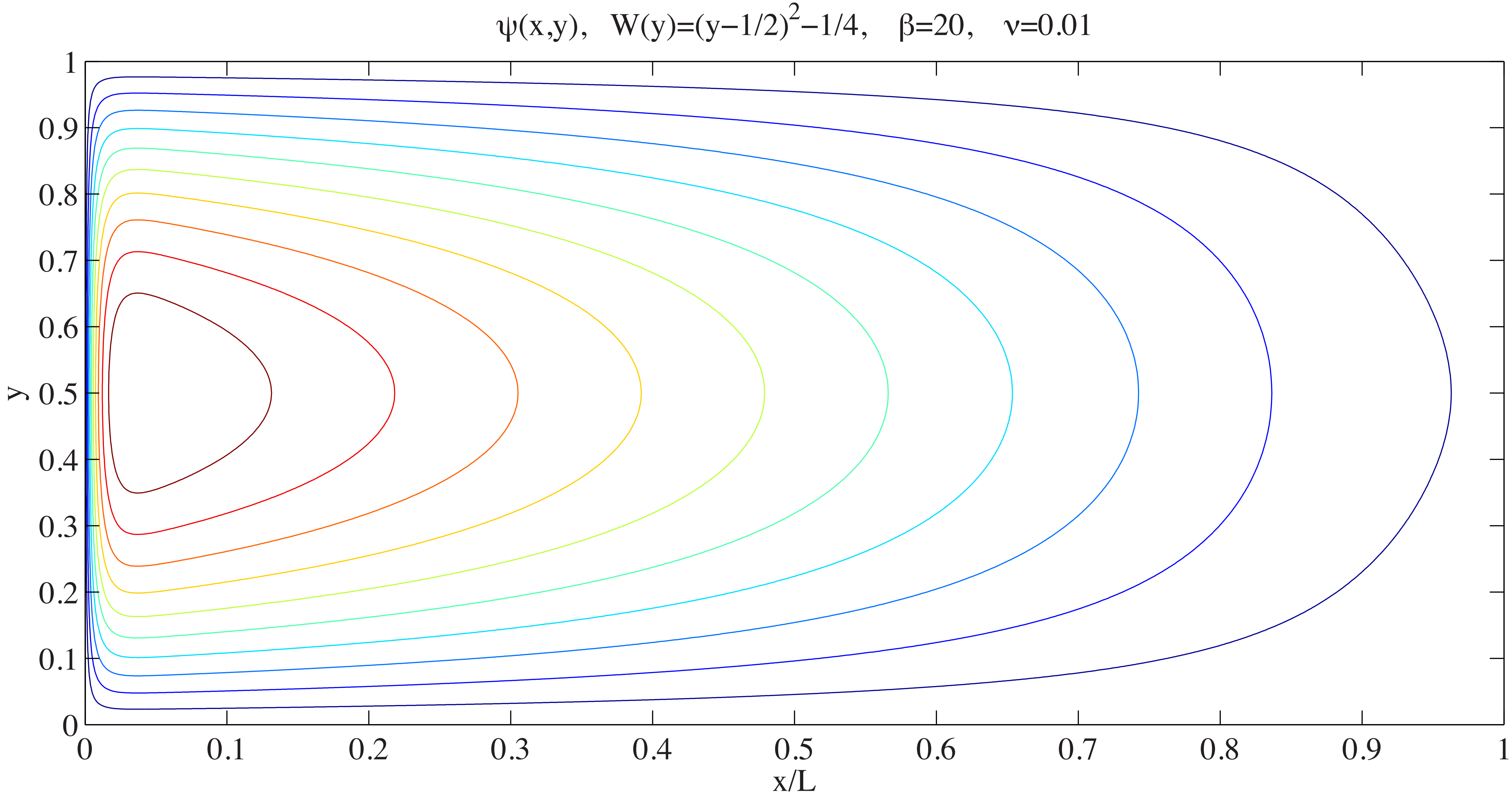
ψ(x,y), W(y)=(y−1/2)^2−1/4, β=20, ν=0.01
y
x/L
0
0.1
0.2
0.3
0.4
0.5
0.6
0.7
0.8
0.9
1

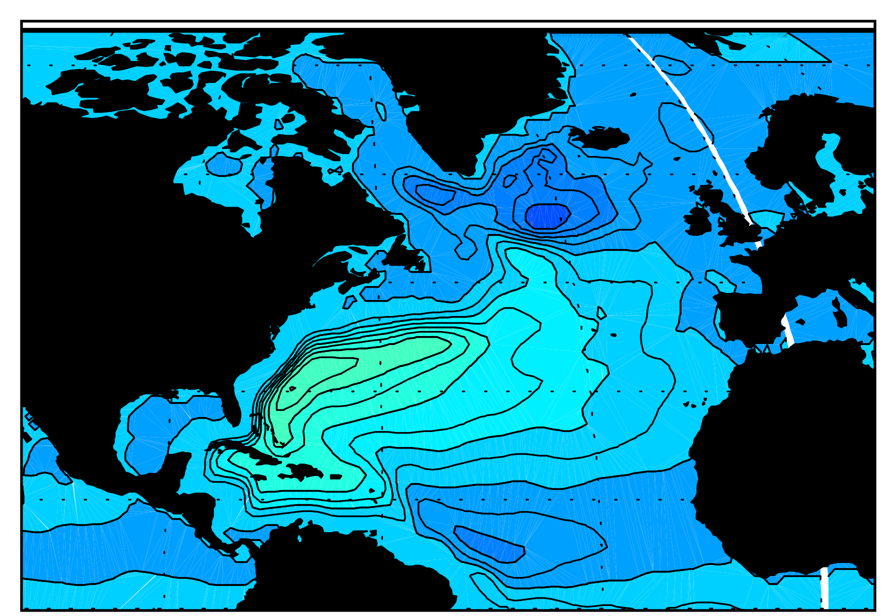

Wind Forcing

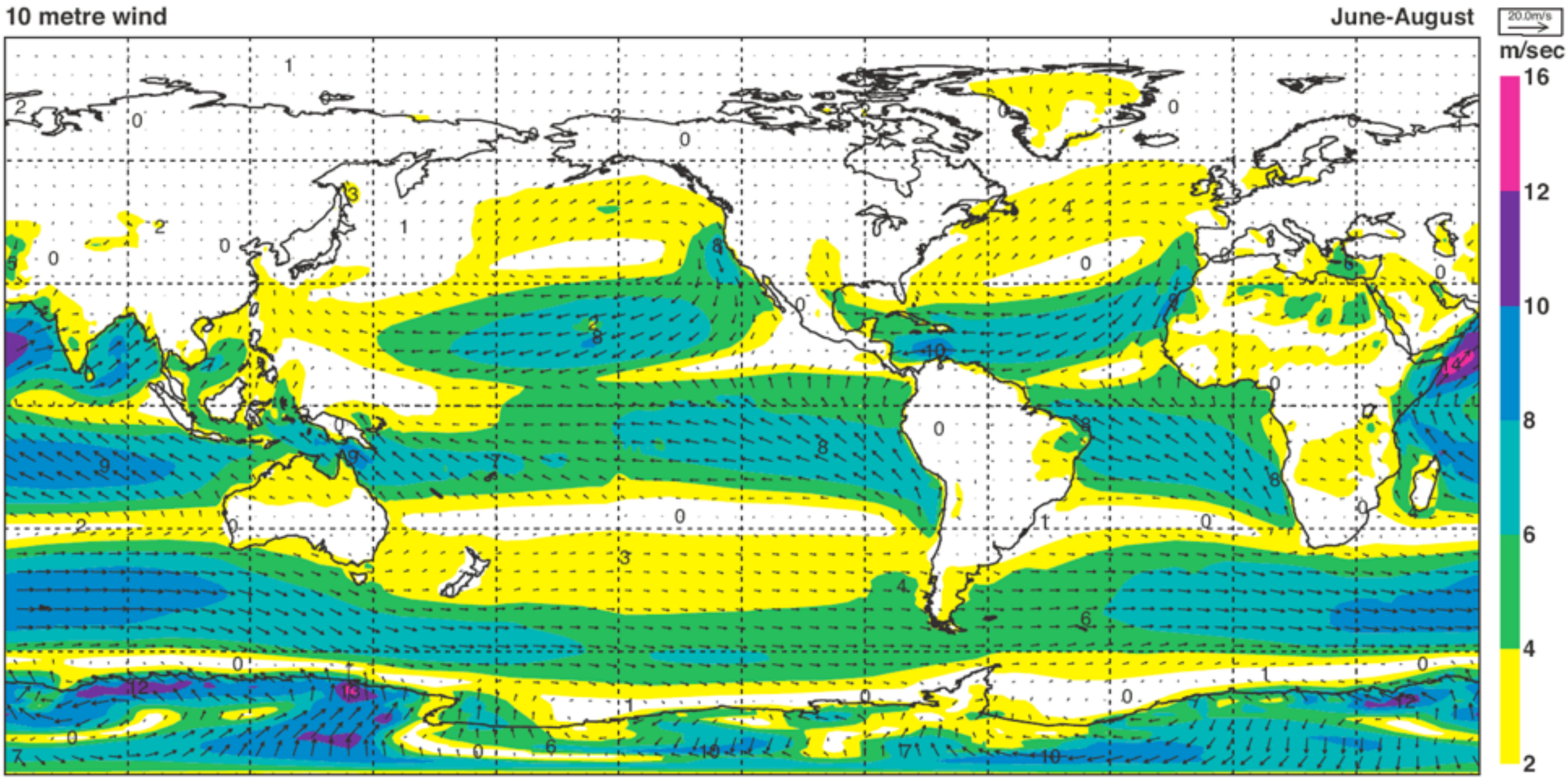

Kallberg et al. 1995 (ERA-40 reanalysis)

Ocean Currents

Time-averaged (16-year) ocean circulation

Wunsch, 2011

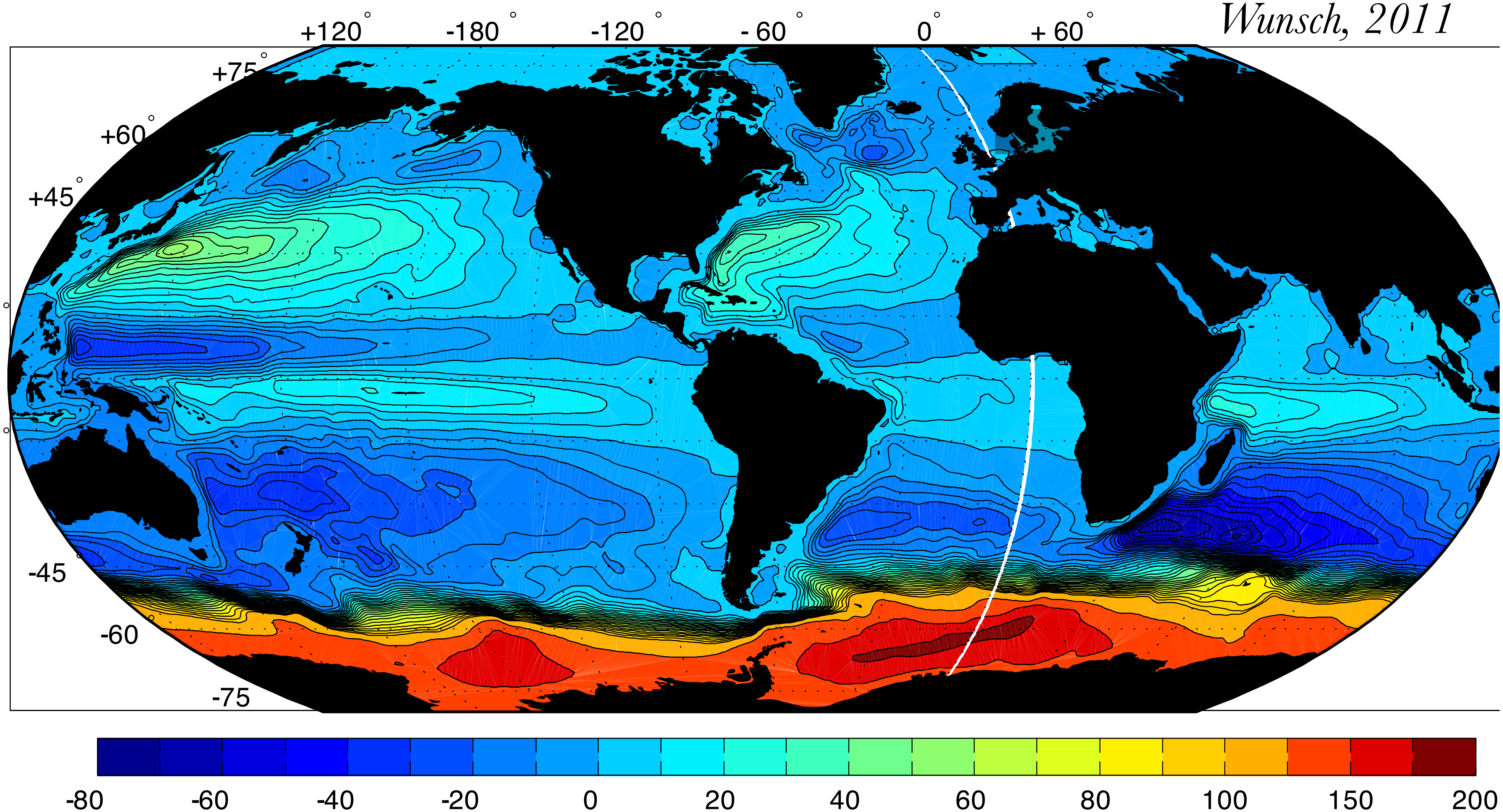

Transport streamfunction (10^6 m^3/s = 1 Sverdrup)

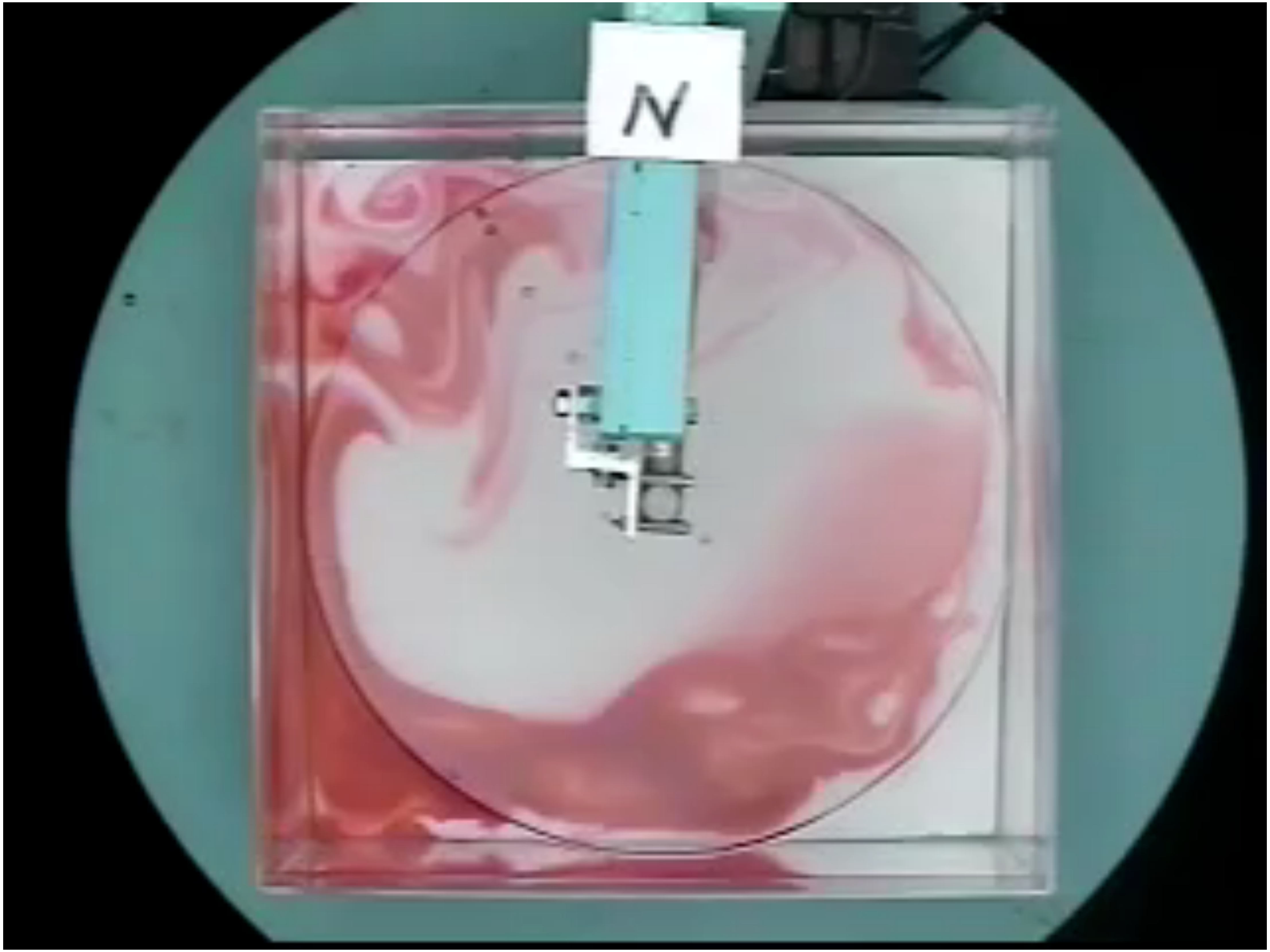
N

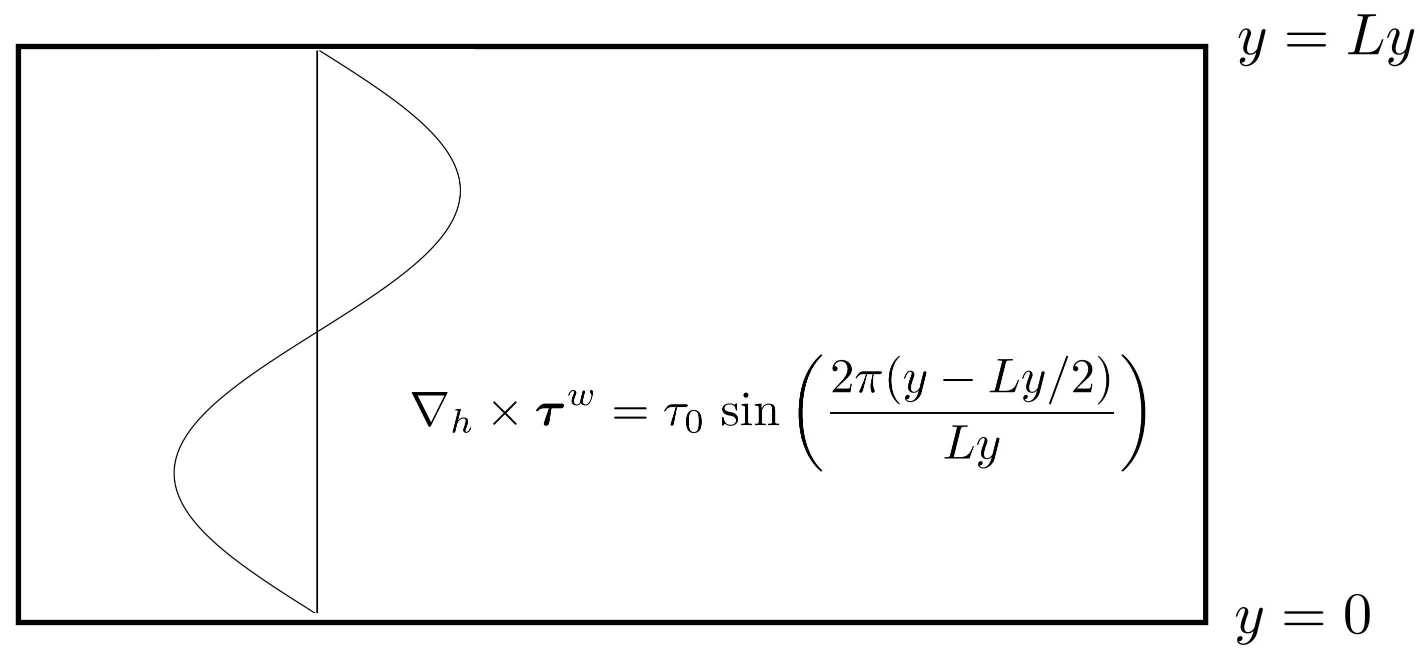

<u>Numerical Simulations:</u>

Time-averaged $\overline{\psi}$ Instantaneous ψ

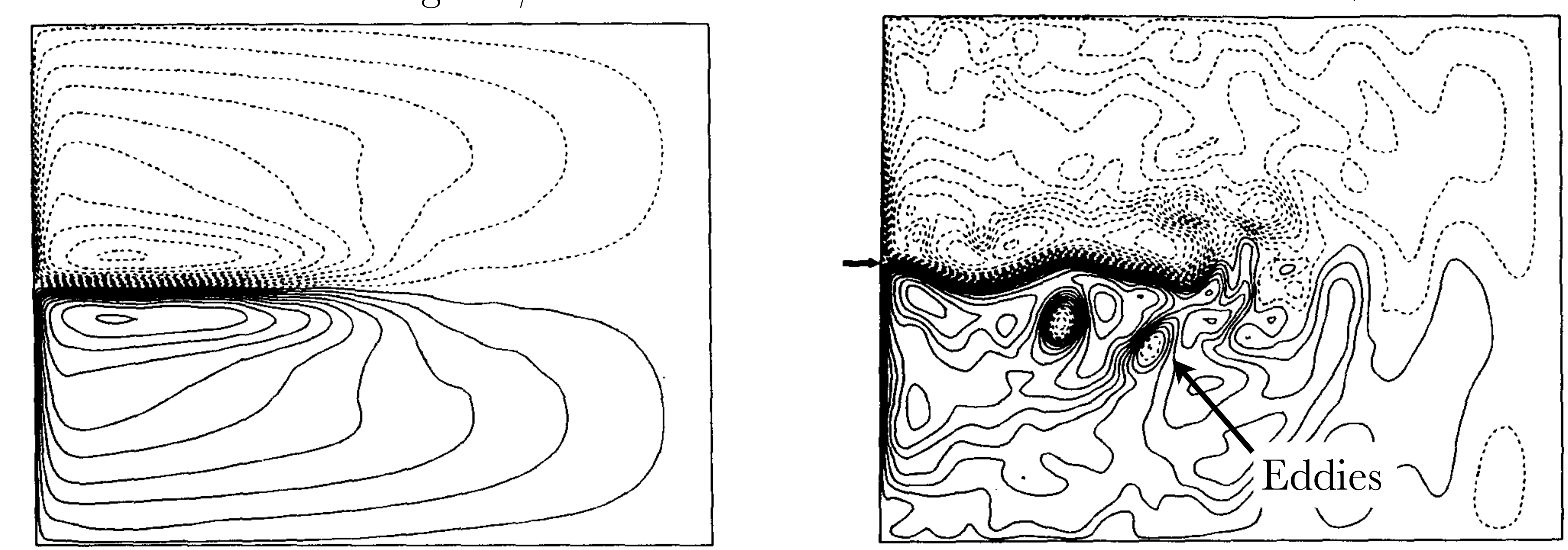

Haidvogel, McWilliams, Gent, J. Phys. Oceanography 1992

Instantaneous ψ

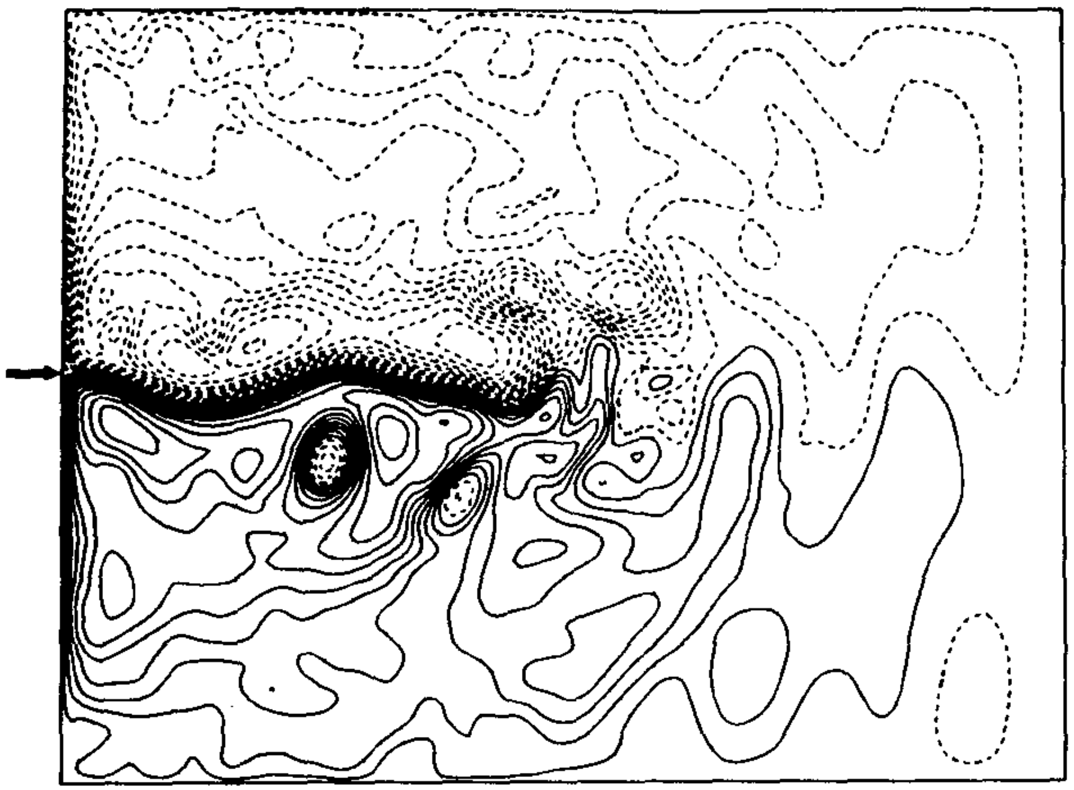

Haidvogel, McWilliams, Gent, J. Phys. Oceanography 1992

Sea-surface temperature

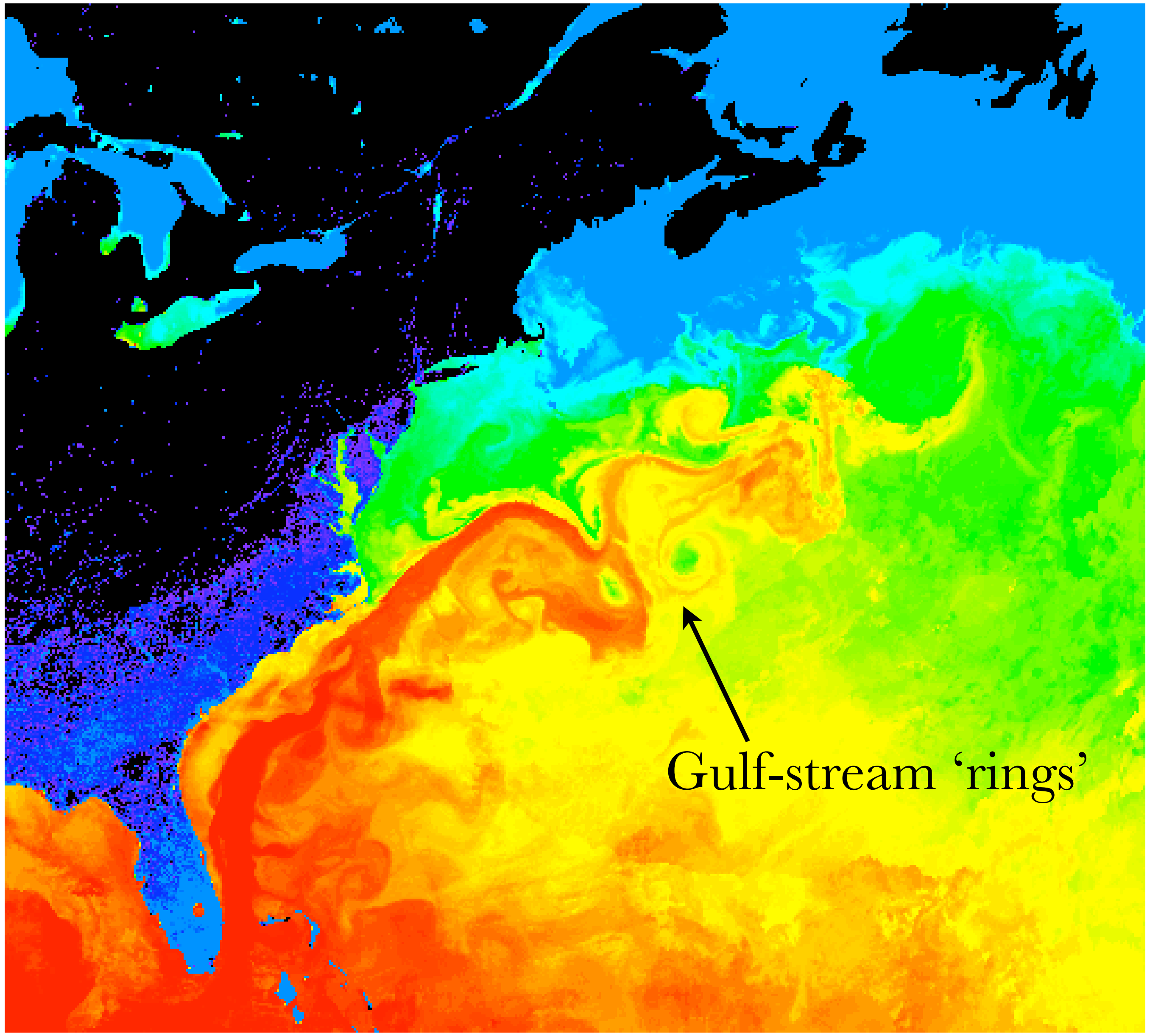

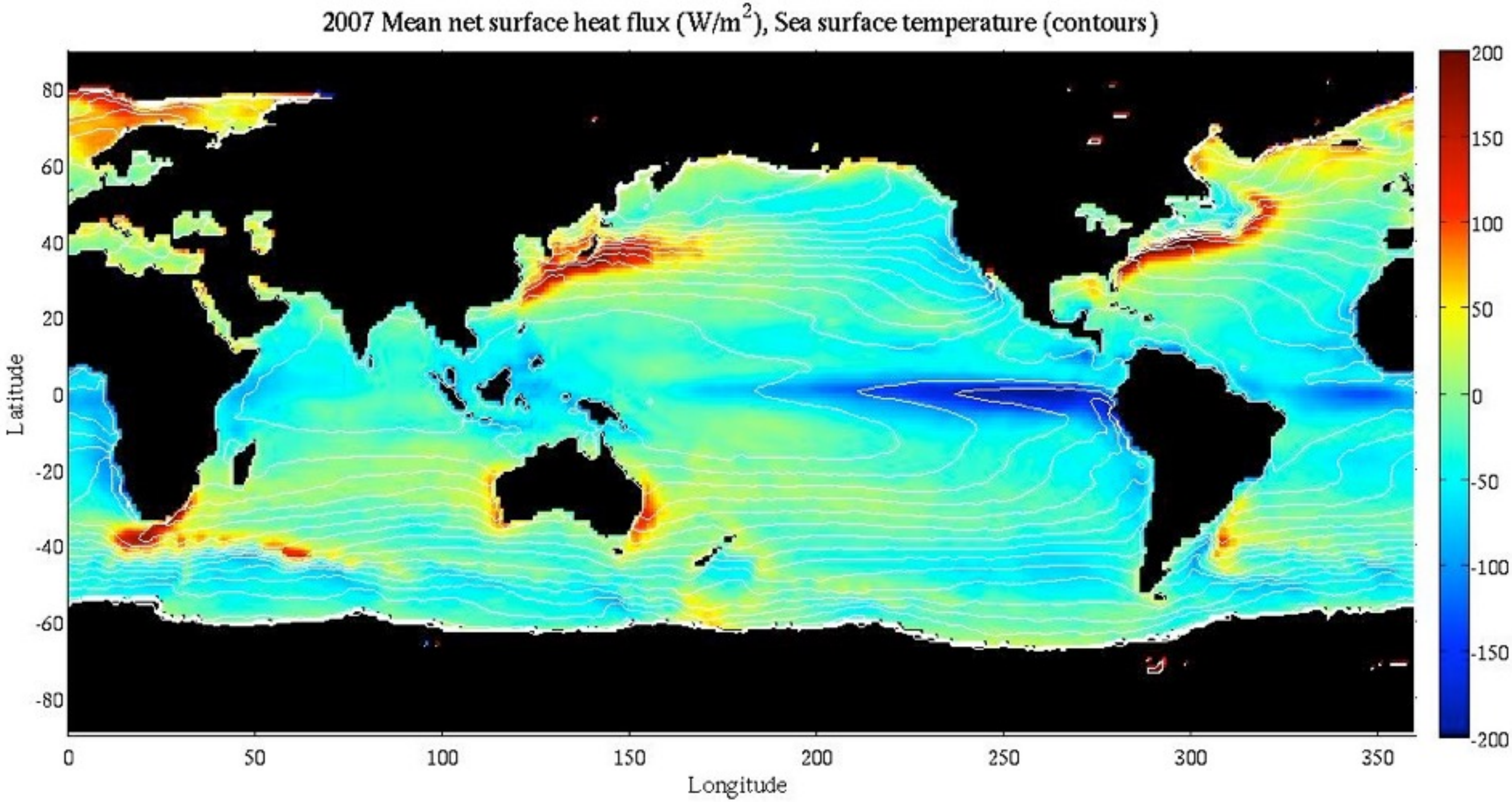

2007 Mean net surface heat flux (W/m²), Sea surface temperature (contours)
80
60
40
20
0
-20
-40
-60
-80
Latitude
0
50
100
150
200
250
300
350
Longitude
200
150
100
50
0
-50
-100
-150
-200

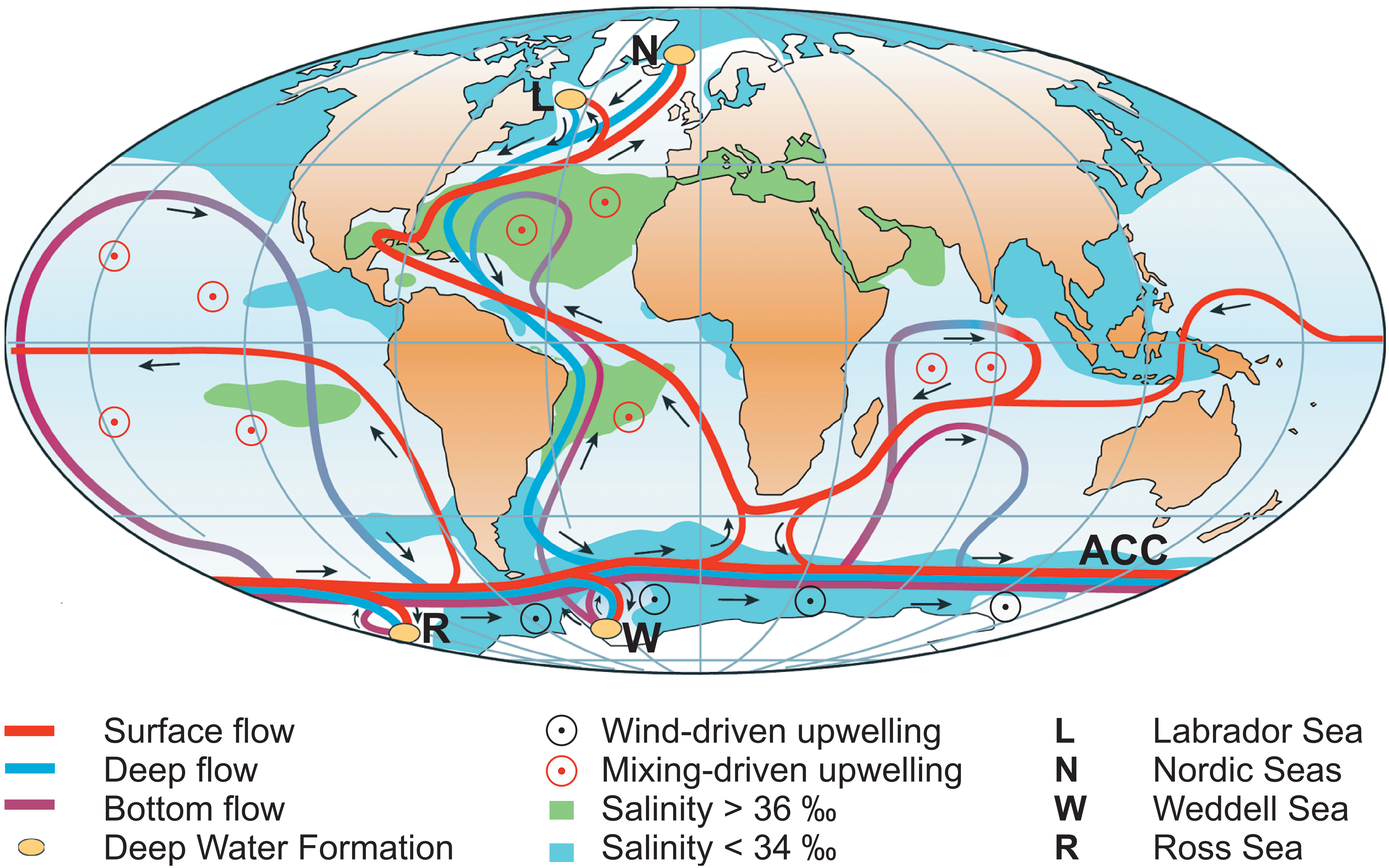
N
L
ACC
R
W
Surface flow
Deep flow
Bottom flow
Deep Water Formation
Wind-driven upwelling
Mixing-driven upwelling
Salinity > 36 ‰
Salinity < 34 ‰
L Labrador Sea
N Nordic Seas
W Weddell Sea
R Ross Sea

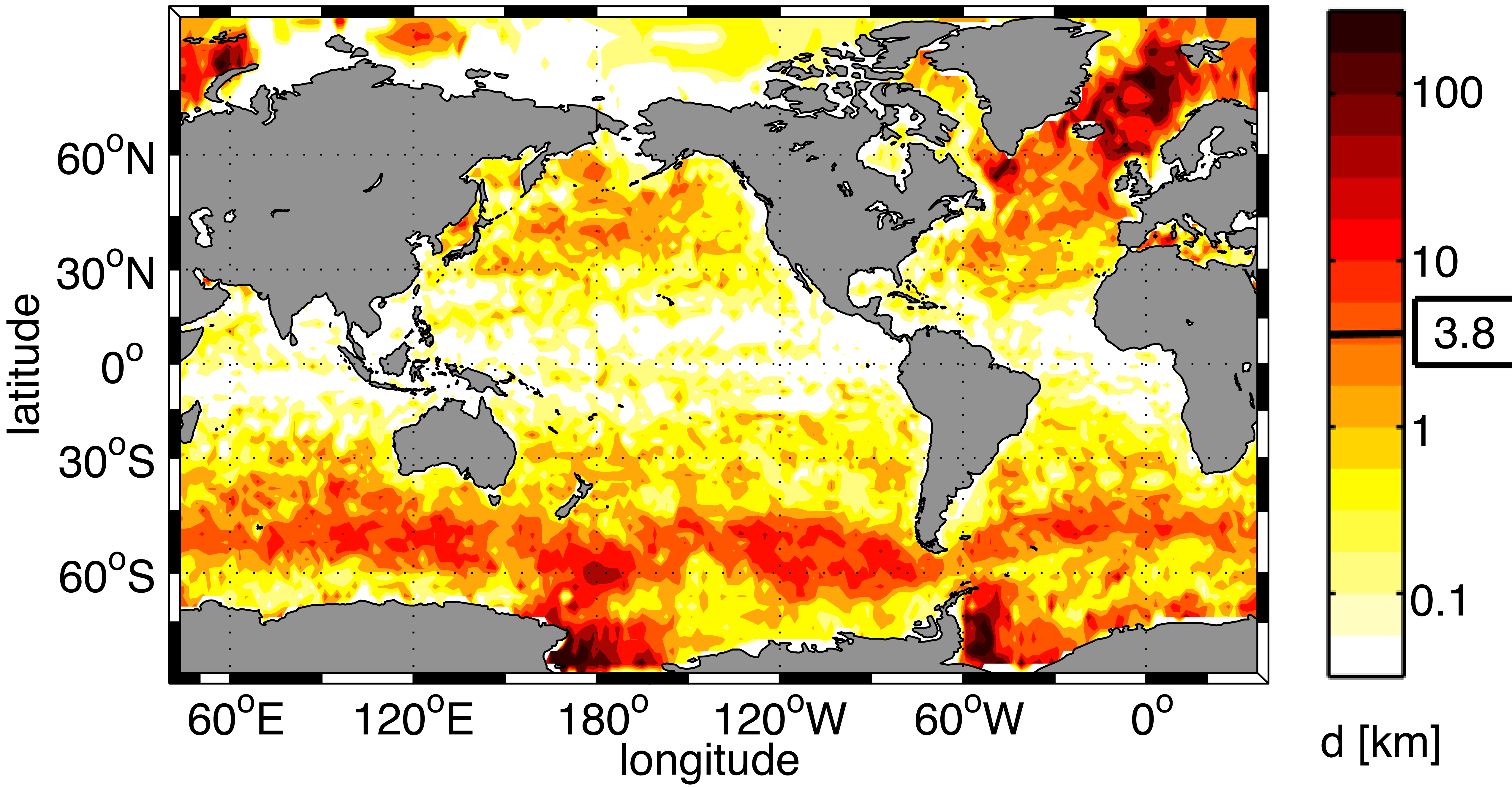

The surface sources of global ocean waters. Oceanic volume that has originated in each 2° by 2° surface location (11,113 origination sites), scaled by the surface area of each box to make an equivalent thickness, d. The color-scale follows a base ten logarithm of the field.

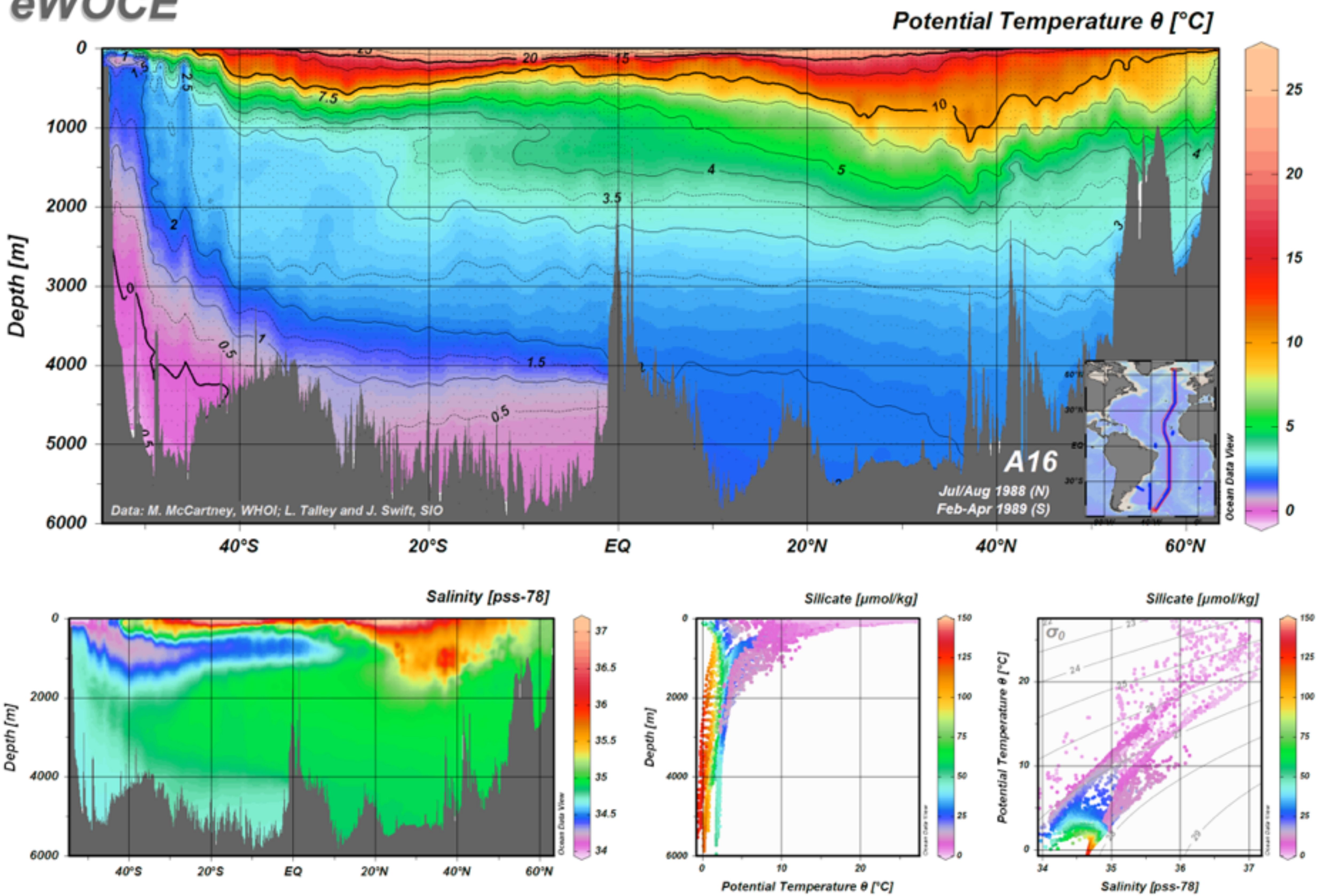
Potential Temperature θ [°C]
Depth [m]
A16
Jul/Aug 1988 (N)
Feb-Apr 1989 (S)
Data: M. McCartney, WHOI; L. Talley and J. Swift, SIO
40°S
20°S
EQ
20°N
40°N
60°N
Ocean Data View
Salinity [pss-78]
Silicate [µmol/kg]
Potential Temperature θ [°C]
Salinity [pss-78]

eWOCE

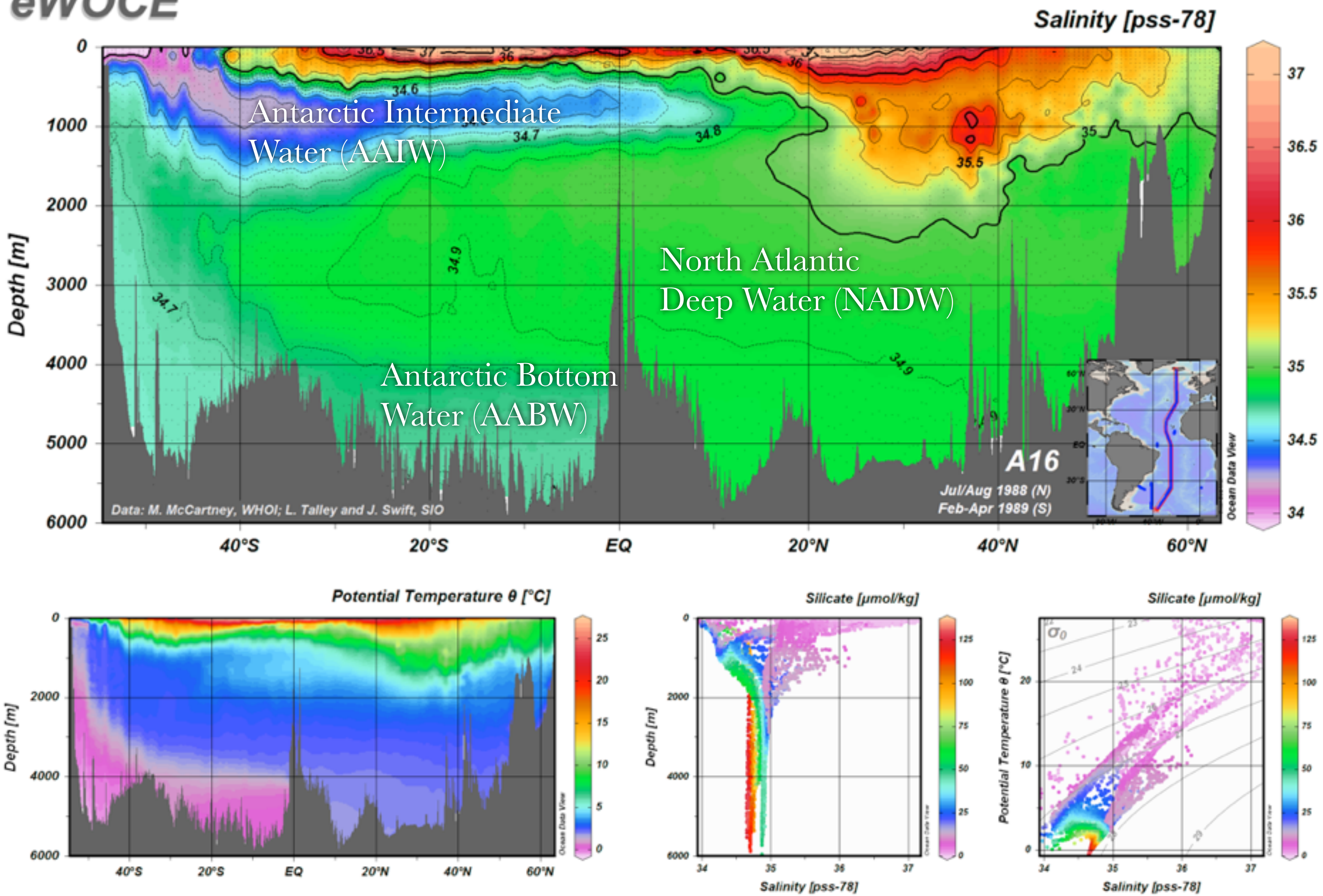

Salinity [pss-78]
Antarctic Intermediate Water (AAIW)
North Atlantic Deep Water (NADW)
Antarctic Bottom Water (AABW)
Depth [m]
A16
Jul/Aug 1988 (N)
Feb-Apr 1989 (S)
Data: M. McCartney, WHOI; L. Talley and J. Swift, SIO
40°S
20°S
EQ
20°N
40°N
60°N
Ocean Data View
Potential Temperature θ [°C]
Silicate [µmol/kg]
Salinity [pss-78]
Potential Temperature θ [°C]

eWOCE

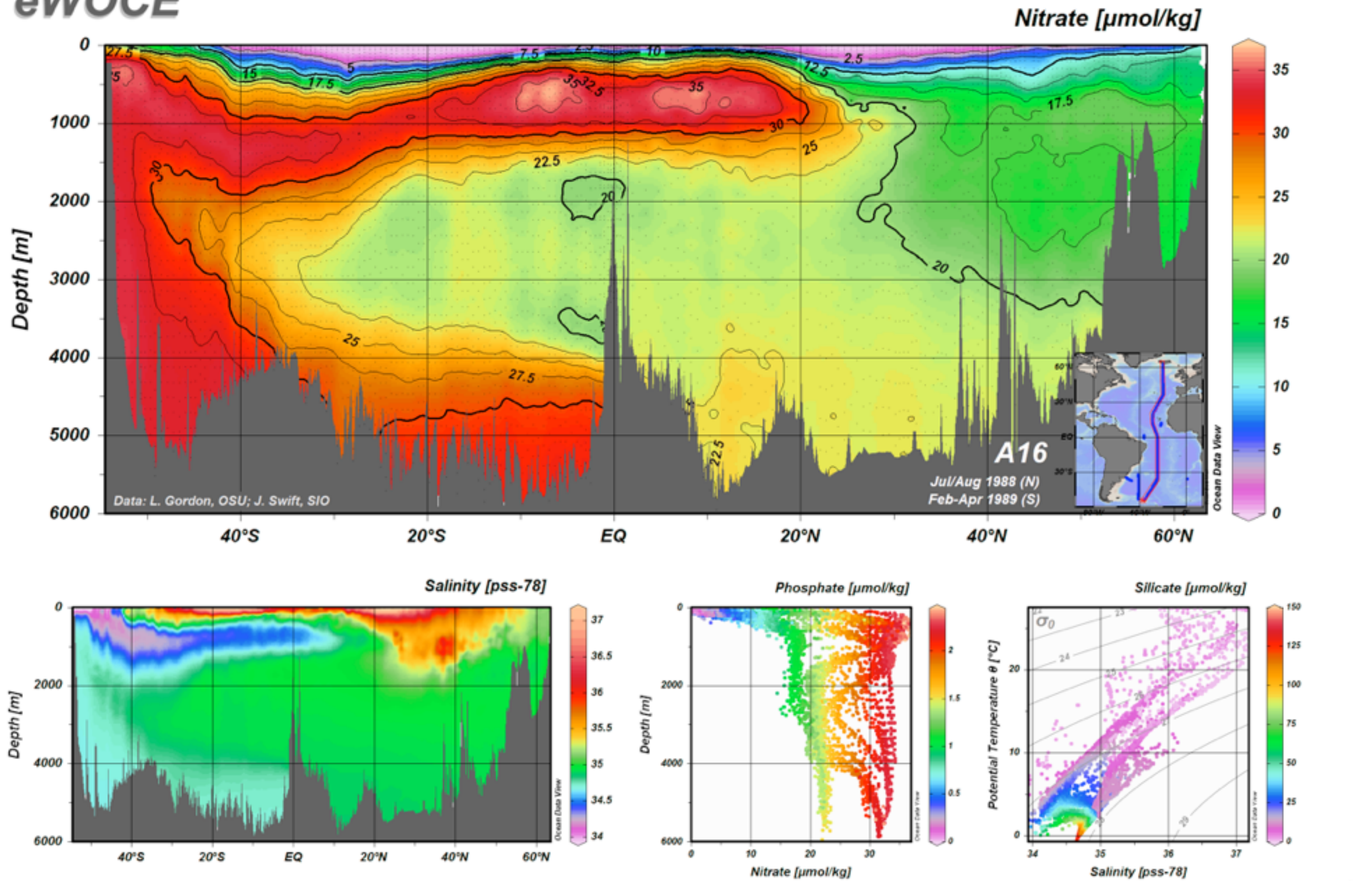

Nitrate [µmol/kg]
Depth [m]
A16
Jul/Aug 1988 (N)
Feb-Apr 1989 (S)
Data: L. Gordon, OSU; J. Swift, SIO
40°S
20°S
EQ
20°N
40°N
60°N
Ocean Data View
Salinity [pss-78]
Phosphate [µmol/kg]
Nitrate [µmol/kg]
Silicate [µmol/kg]
Potential Temperature θ [°C]
Salinity [pss-78]

Averaging, across an ocean in longitude

- Meridional Overturning Circulation (MOC)
  (sometimes called the Thermohaline Circulation, THC)

Atlantic MOC (1 Sv = 10^6 m^3/s)

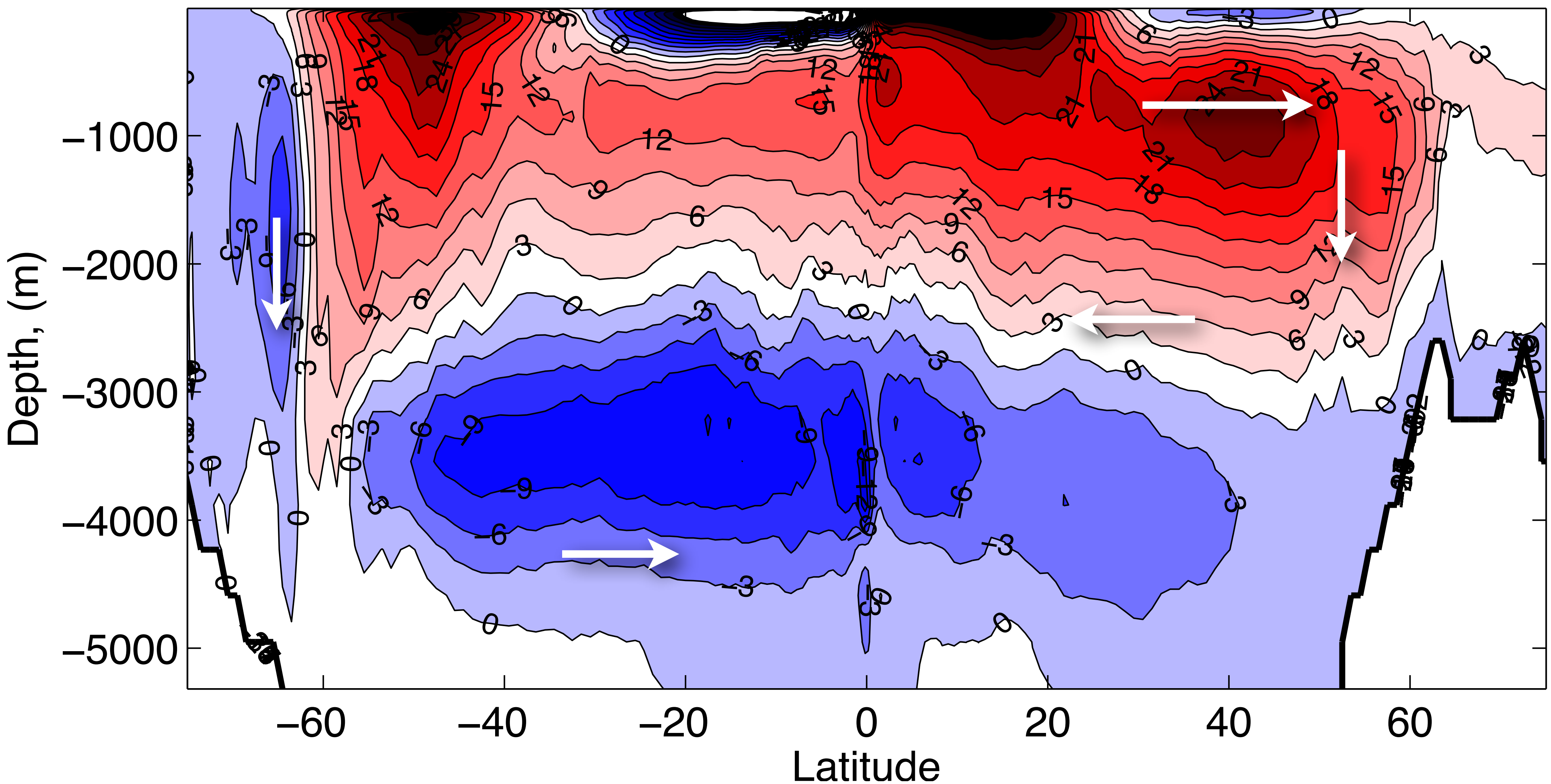

Nikurashin and Vallis, 2011

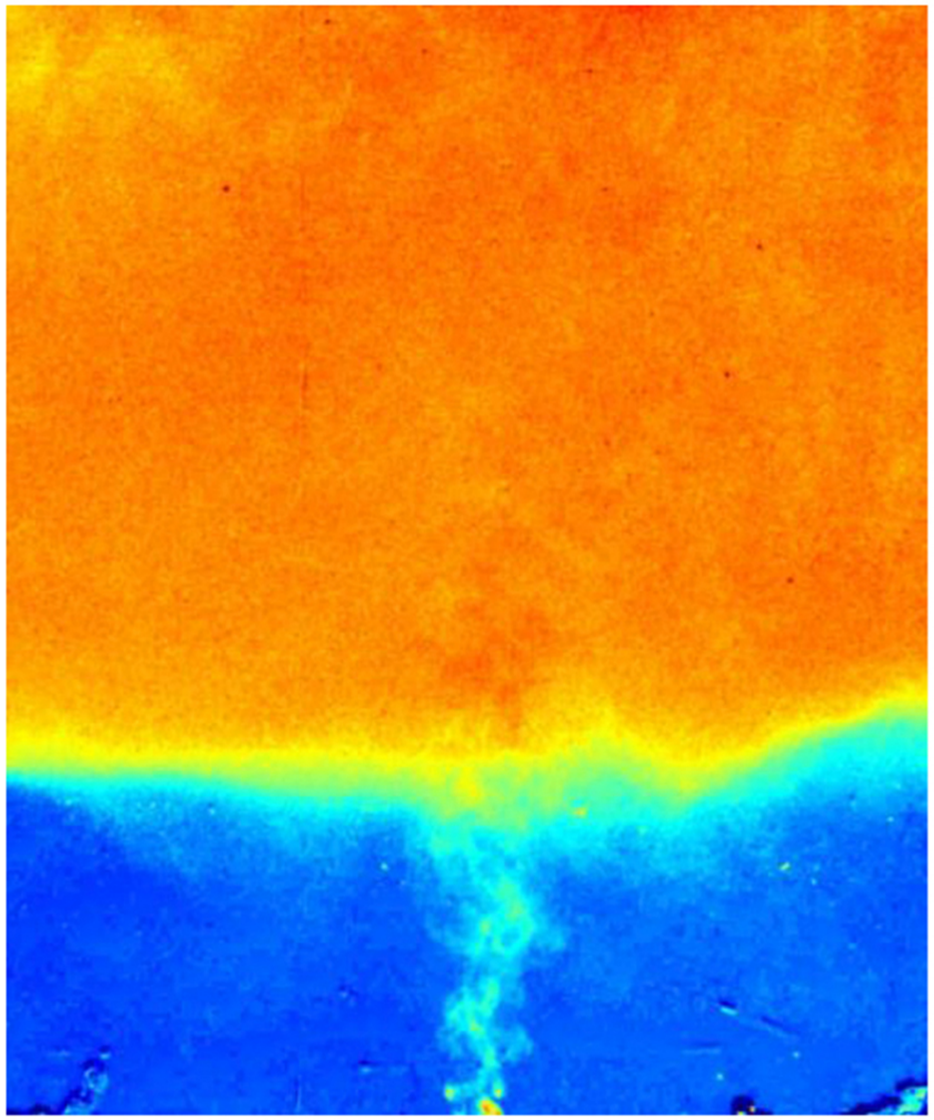

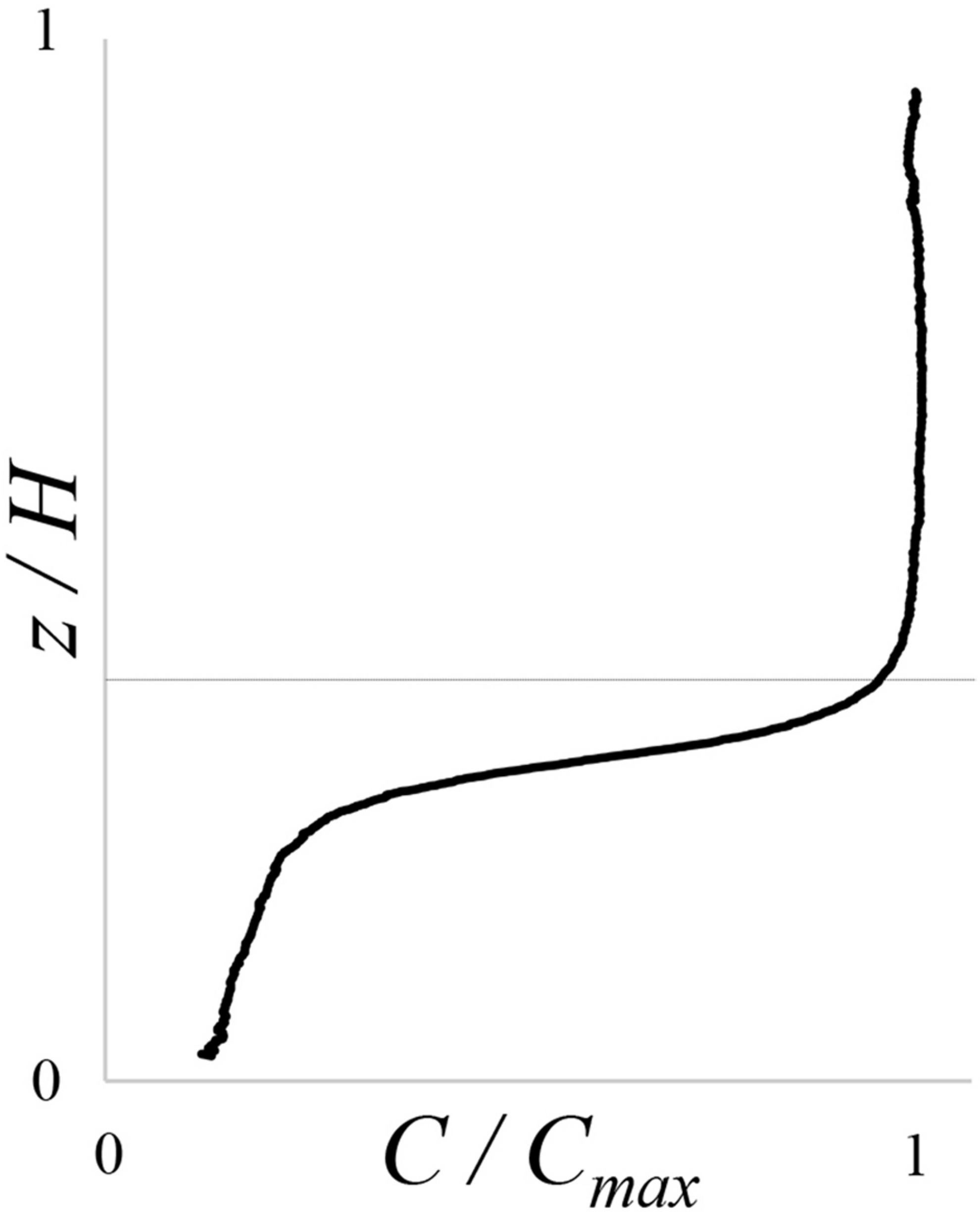

Mignotti + Woods, 2015

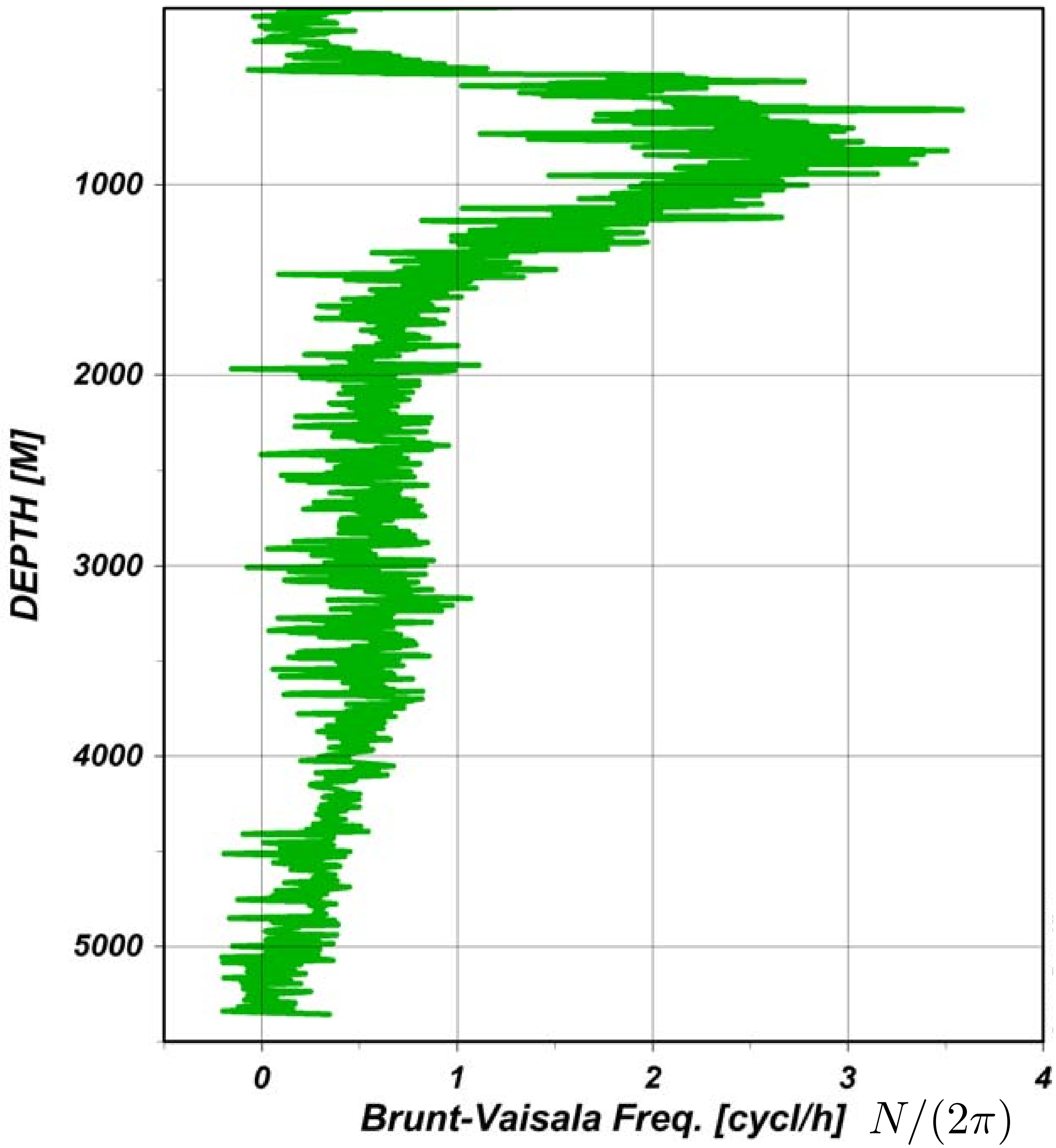

Mixed layer

Thermocline

Abyss

$N/(2\pi)$

$$N^2 = -\frac{g}{\rho_0}\frac{\partial \rho}{\partial z}$$

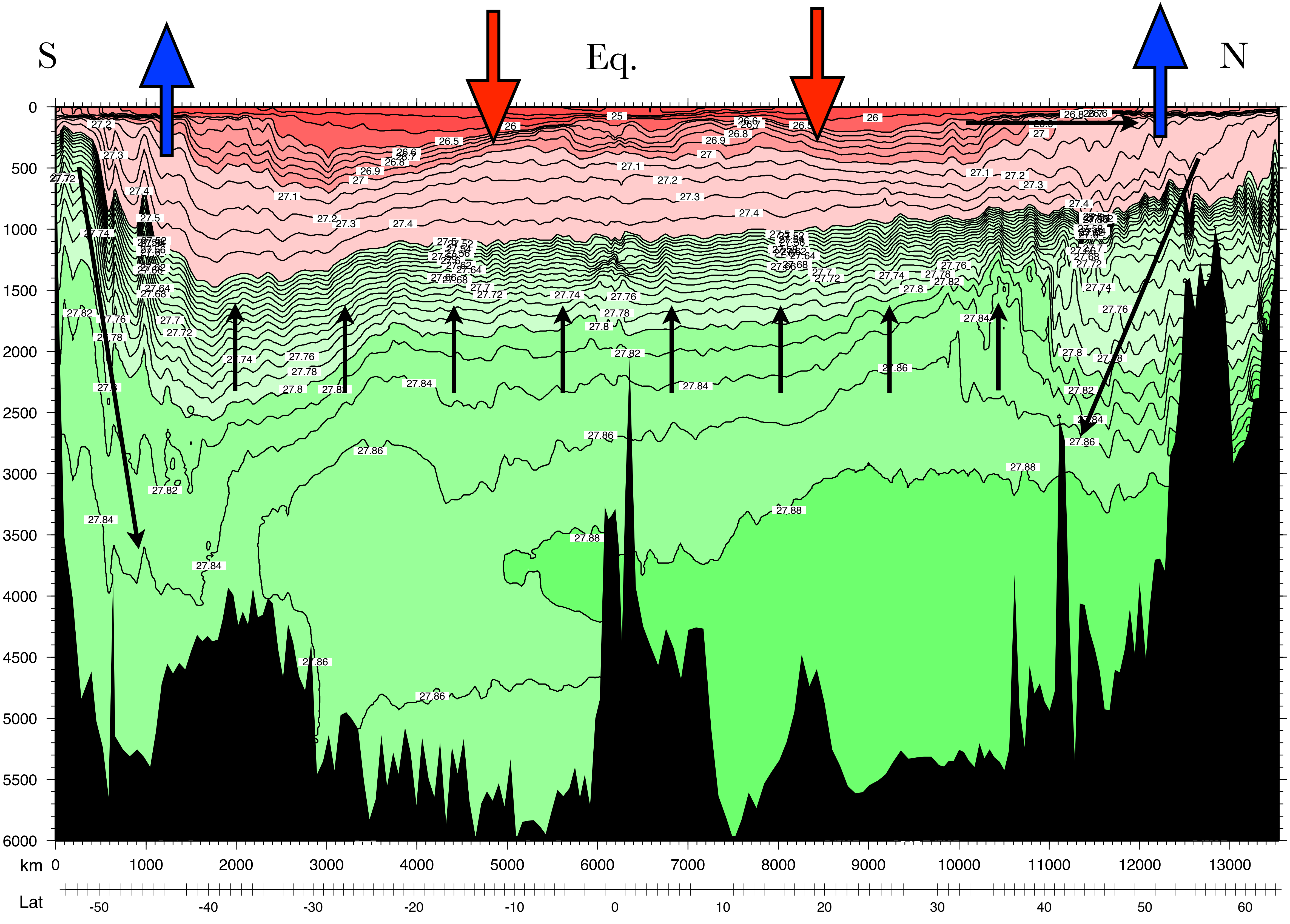

S
Eq.
N
km
Lat

‘Missing’ Mixing

Problem: Observations of ocean mixing typically find $\kappa \approx 10^{-5}\ m^2/s \ << 10^{-4}\ m^2/s$

Inferred diffusivity, North-South Atlantic section

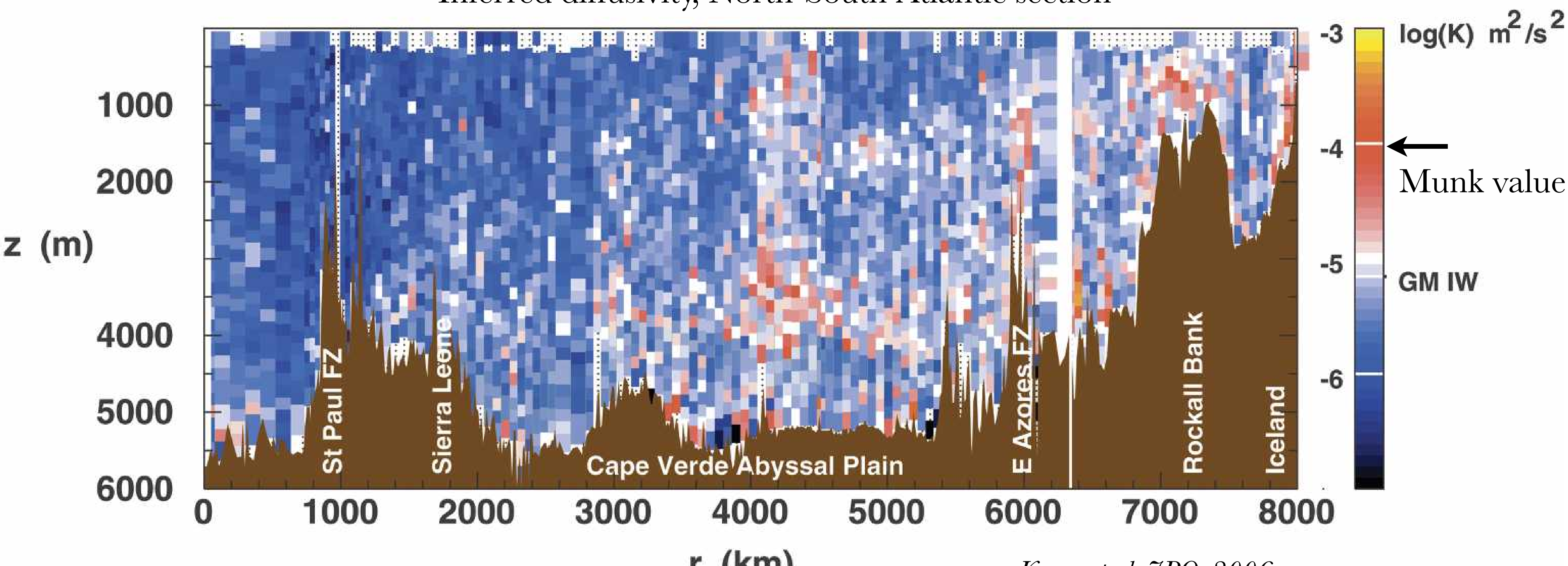

Kunze et al. JPO, 2006

Evidence for slow mixing across the pycnocline from an open-ocean tracer-release experiment

James R. Ledwell*, Andrew J. Watson† & Clifford S. Law†

* Applied Ocean Physics and Engineering, Woods Hole Oceanographic Institution, Woods Hole, Massachusetts 02543, USA
† Plymouth Marine Laboratory, Prospect Place, West Hoe, Plymouth PL1 3DH, UK

The distributions of heat, salt and trace substances in the ocean thermocline depend on mixing along and across surfaces of equal density (isopycnal and diapycnal mixing, respectively). Measurements of the invasion of anthropogenic tracers, such as bomb tritium and ^{3}He (see, for example, refs 1 and 2), have indicated that isopycnal processes dominate diapycnal mixing, and turbulence measurements have suggested that diapycnal mixing is small[3,4], but it has not been possible to measure accurately the diapycnal diffusivity. Here we report such a measurement, obtained from the vertical dispersal of a patch of the inert compound SF_6 released in the open ocean. The diapycnal diffusivity, averaged over hundreds of kilometres and five months, was $0.11 \pm 0.02\ \mathrm{cm^2\,s^{-1}}$, confirming previous estimates[1–4]. Such a low diffusivity can support only a rather small diapycnal flux of nitrate into the euphotic zone; it justifies the neglect of diapycnal mixing in dynamic models of the thermocline[25–27], and implies that heat, salt and tracers must penetrate the thermocline mostly by transport along, rather than across, density surfaces.

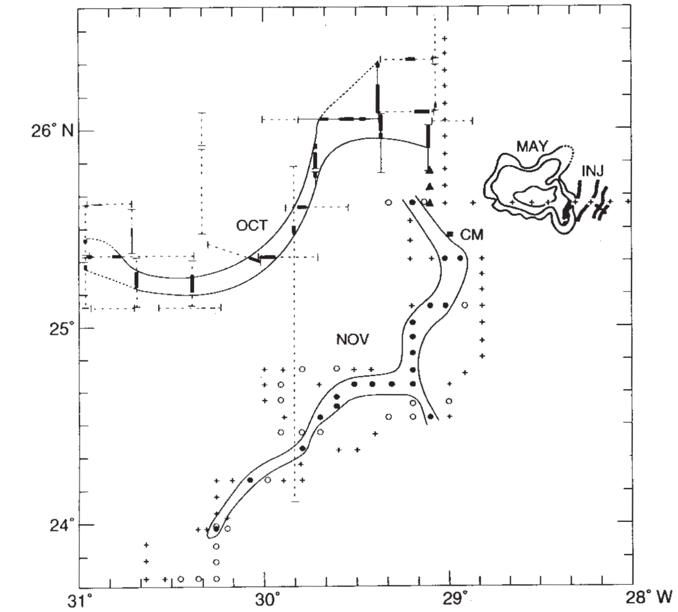

FIG. 1 Evolution of the lateral distribution of the tracer. The injection streaks are shown as short heavy lines near 26° N, 28° W. The contours just to the west show the patch later in May 1992. Heavy lines (further to the west) show tracks for the October survey, where the concentration C at the target surface was >500 fM; light solid lines, C was between 100 and 500 fM; dashed lines, $C \sim 0$. Solid triangles indicate bottle stations occupied at the end of the October cruise, with $C > 300$ fM. Station symbols for the November survey are: plus signs, $C < 30$ fM; open circles, $C = 30$–300 fM; filled circles, $C > 300$ fM. A fine curve has been drawn to envelop the high C regions for the two surveys. CM marks the location of the central mooring for the Subduction experiment.

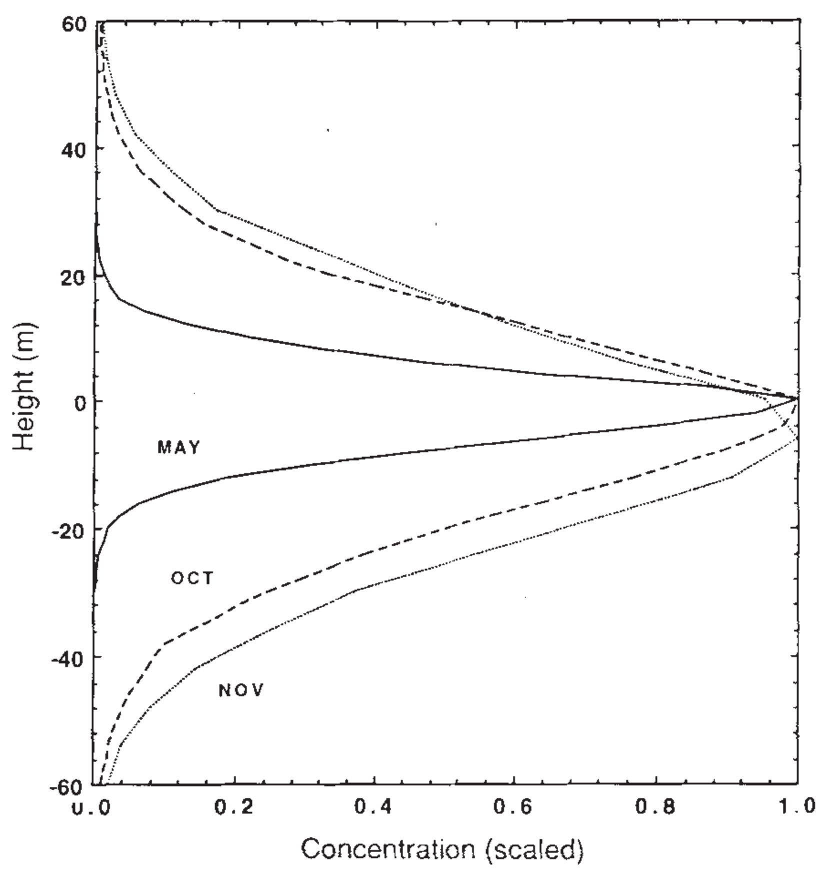

FIG. 2 Evolution of the vertical distribution of the tracer. The mean profiles have been scaled so that the widths can be compared.

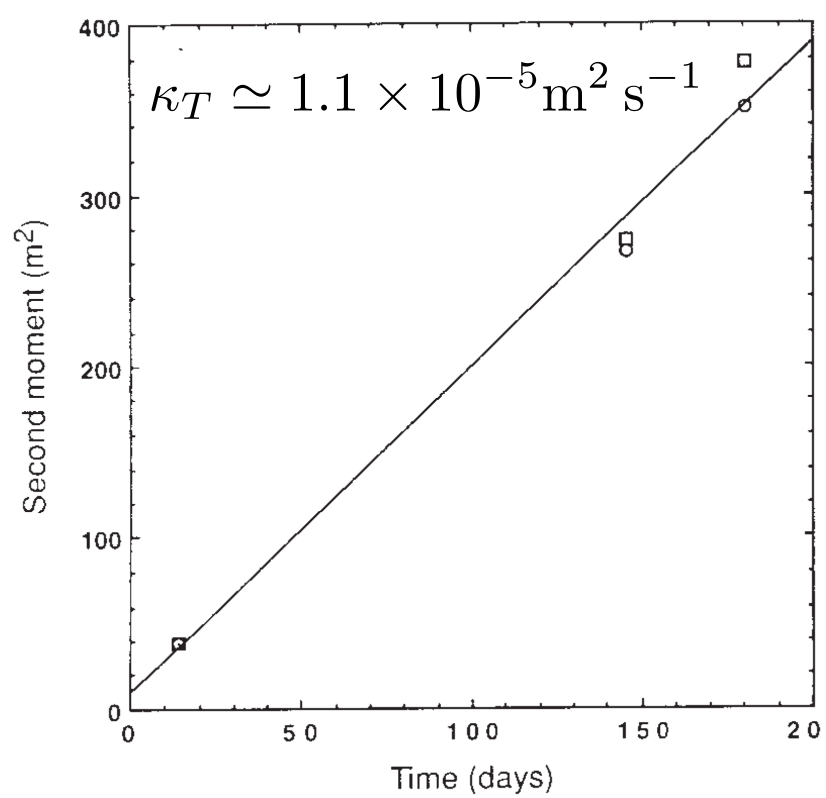

FIG. 3 Growth of the second moment of the vertical tracer distribution. Squares are for raw M_2, circles are for the centre of mass shifted to $h = 0$. The line is for $K_z = 0.11\ \mathrm{cm^2\,s^{-1}}$.

Mixing Efficiency

Inoue + Smyth 2009

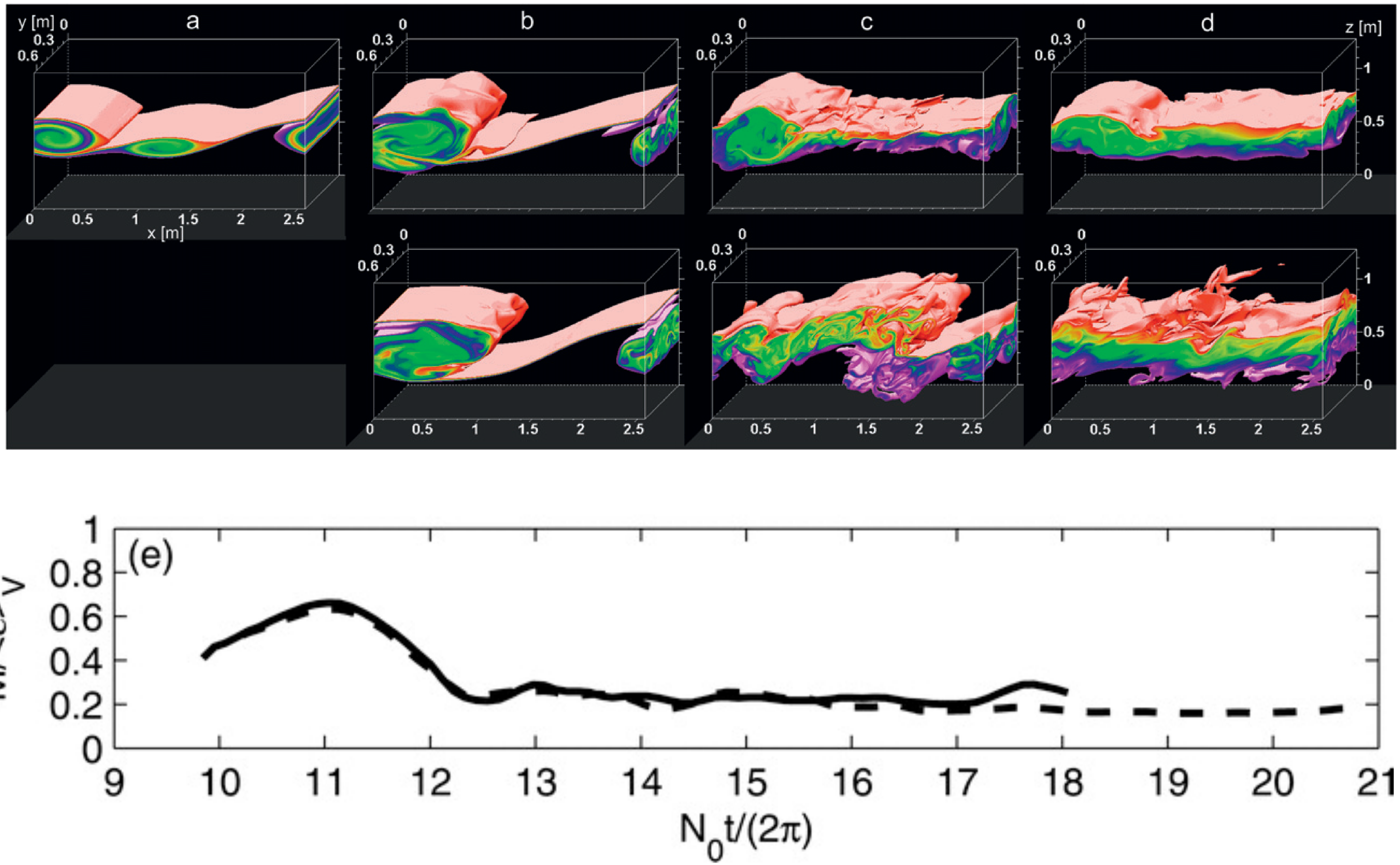

Boundary Mixing

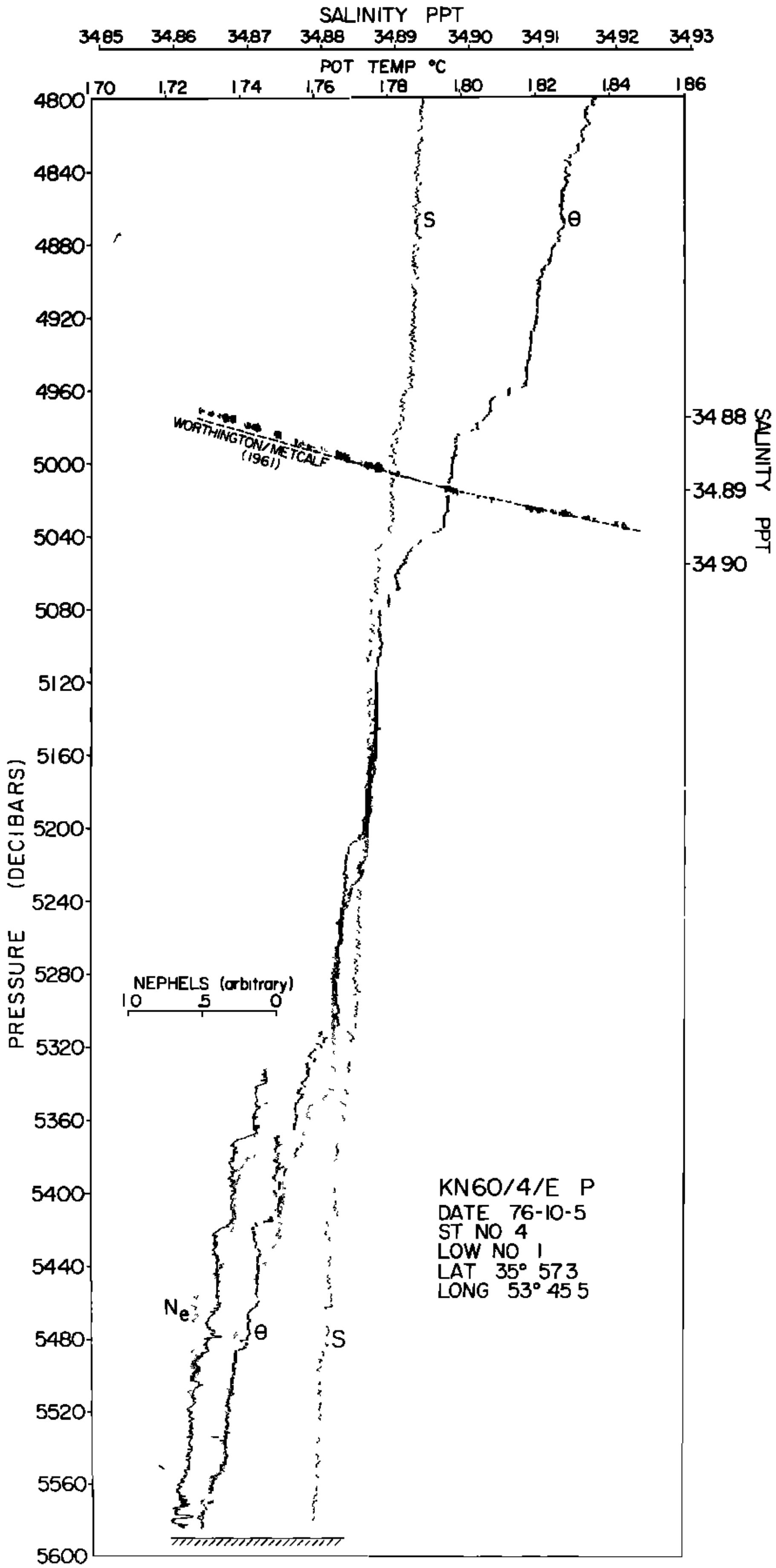

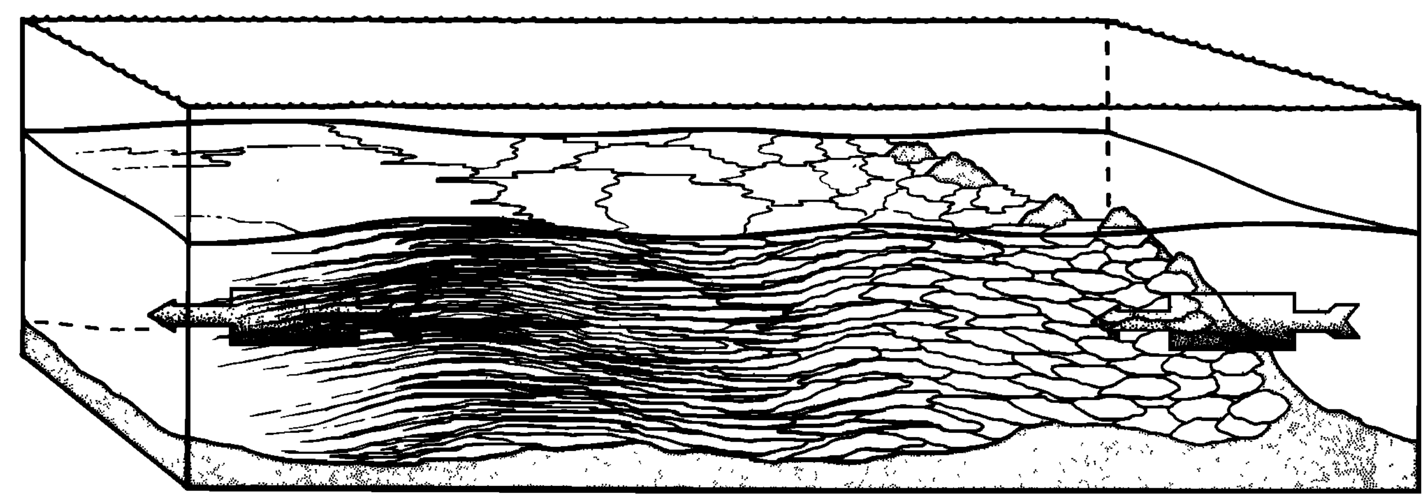

Armi, 1972

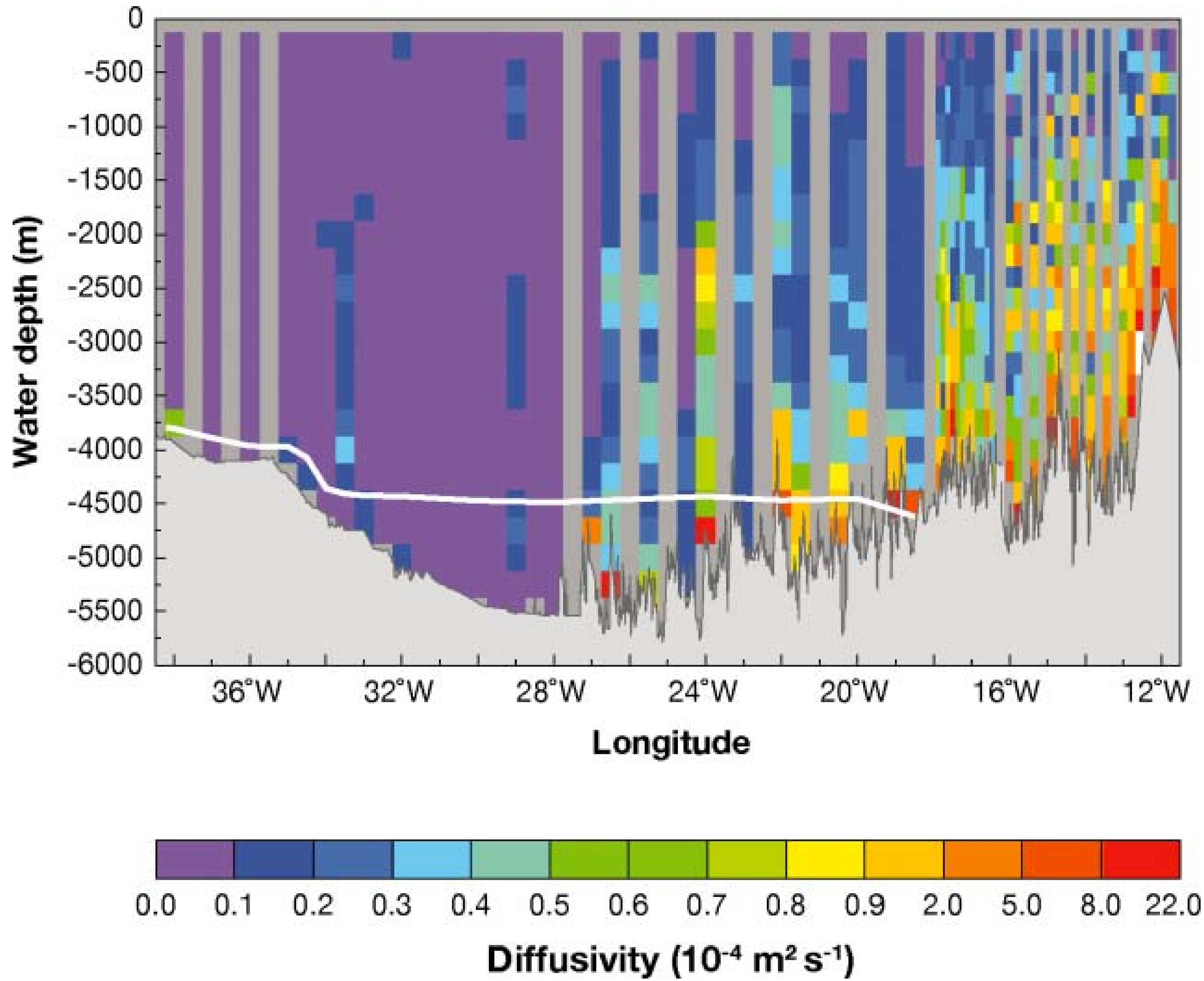

0
-500
-1000
-1500
-2000
-2500
-3000
-3500
-4000
-4500
-5000
-5500
-6000
Water depth (m)
36°W
32°W
28°W
24°W
20°W
16°W
12°W
Longitude
0.0
0.1
0.2
0.3
0.4
0.5
0.6
0.7
0.8
0.9
2.0
5.0
8.0
22.0
Diffusivity (10^{-4} m^2 s^{-1})

Horizontal convection

Hughes and Griffiths 2008

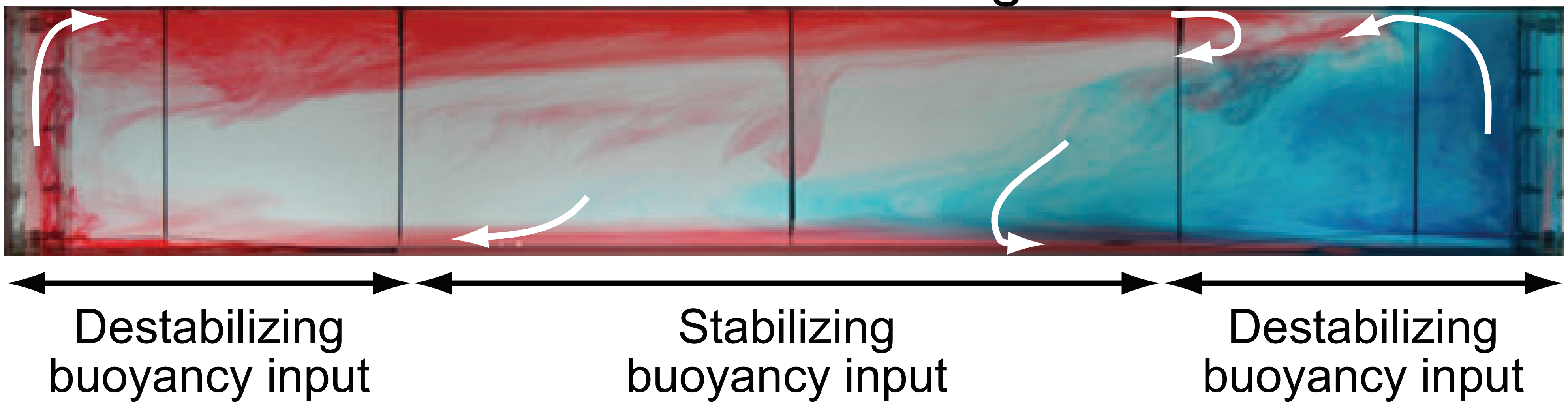

Available Potential Energy and Irreversible Mixing in the Meridional Overturning Circulation

GRAHAM O. HUGHES, ANDREW MCC. HOGG, AND ROSS W. GRIFFITHS

The Australian National University, Canberra, Australia

(d) $K_z = 0.0001\,m^2/s$; $\psi = 28\times10^3$ kg/s; $\Delta\rho = 0.93$ kg/m^3

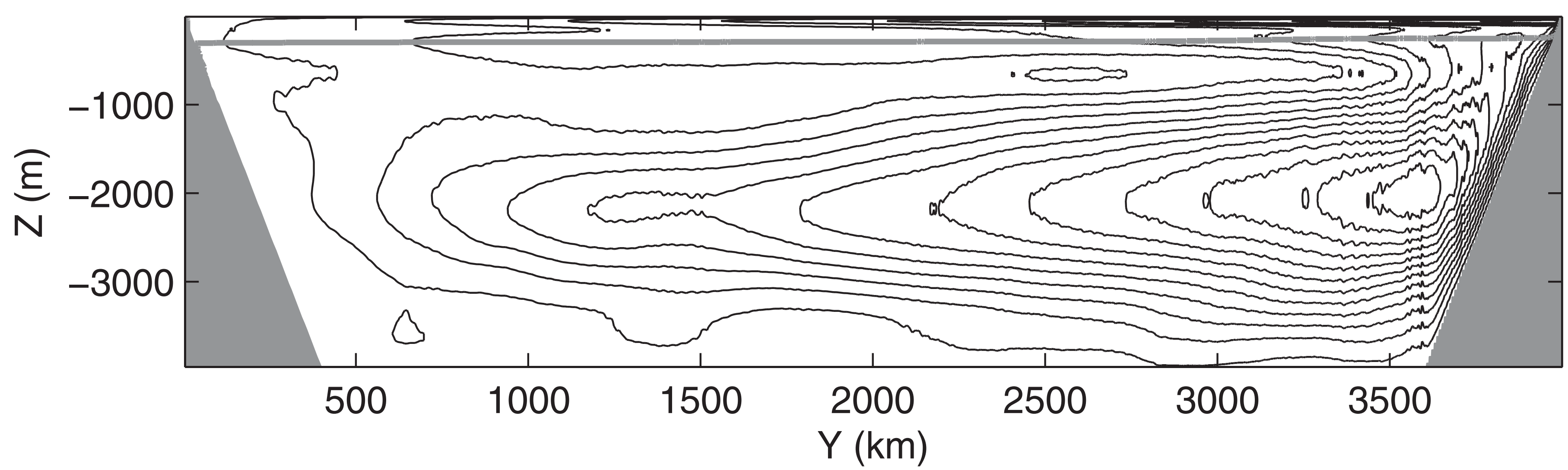

FIG. 4. Dependence of the time-averaged overturning circulation upon the vertical diffusion coefficient (surface buoyancy flux is fixed, with $Q_0 = 200$ W m^{-2}). The maximum streamfunction quoted is that for a two-dimensional flow in a basin of 1-m width, while the density range is $\Delta\rho = \overline{\rho}_{\mathrm{bottom}} - \overline{\rho}_{\mathrm{top}}$. The 20°C isotherm is shown in gray.

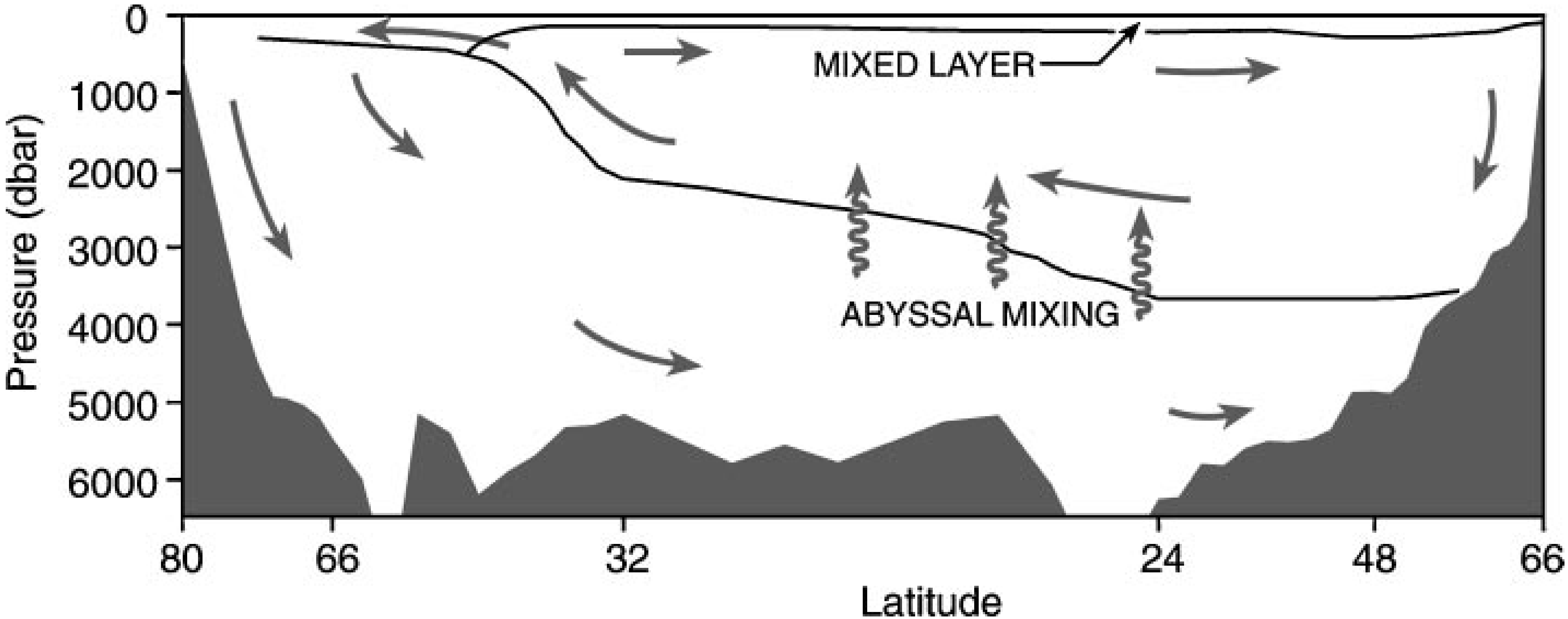

Wunsch and Ferrari, 2004

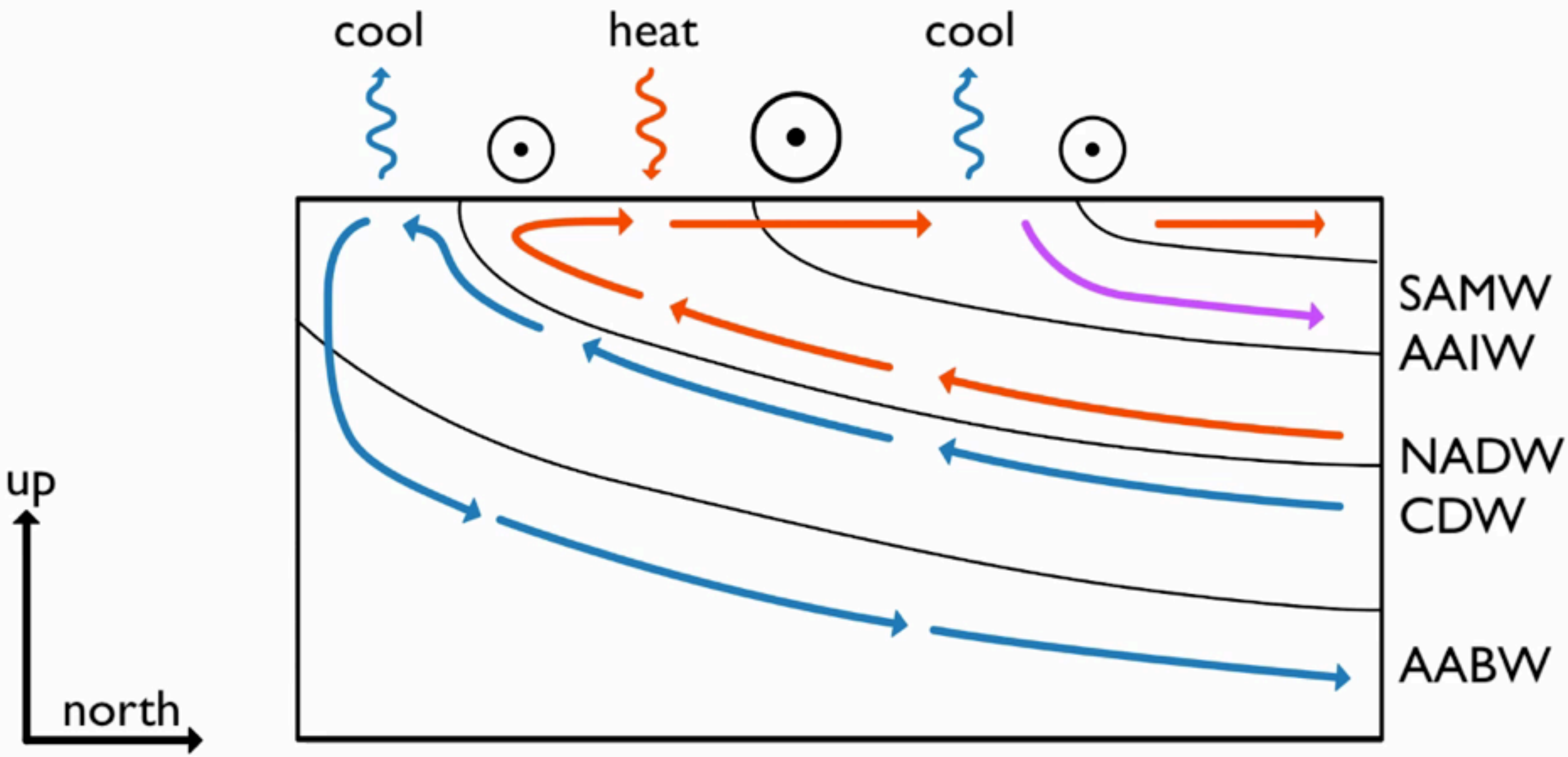

Video: Ryan Abernathy

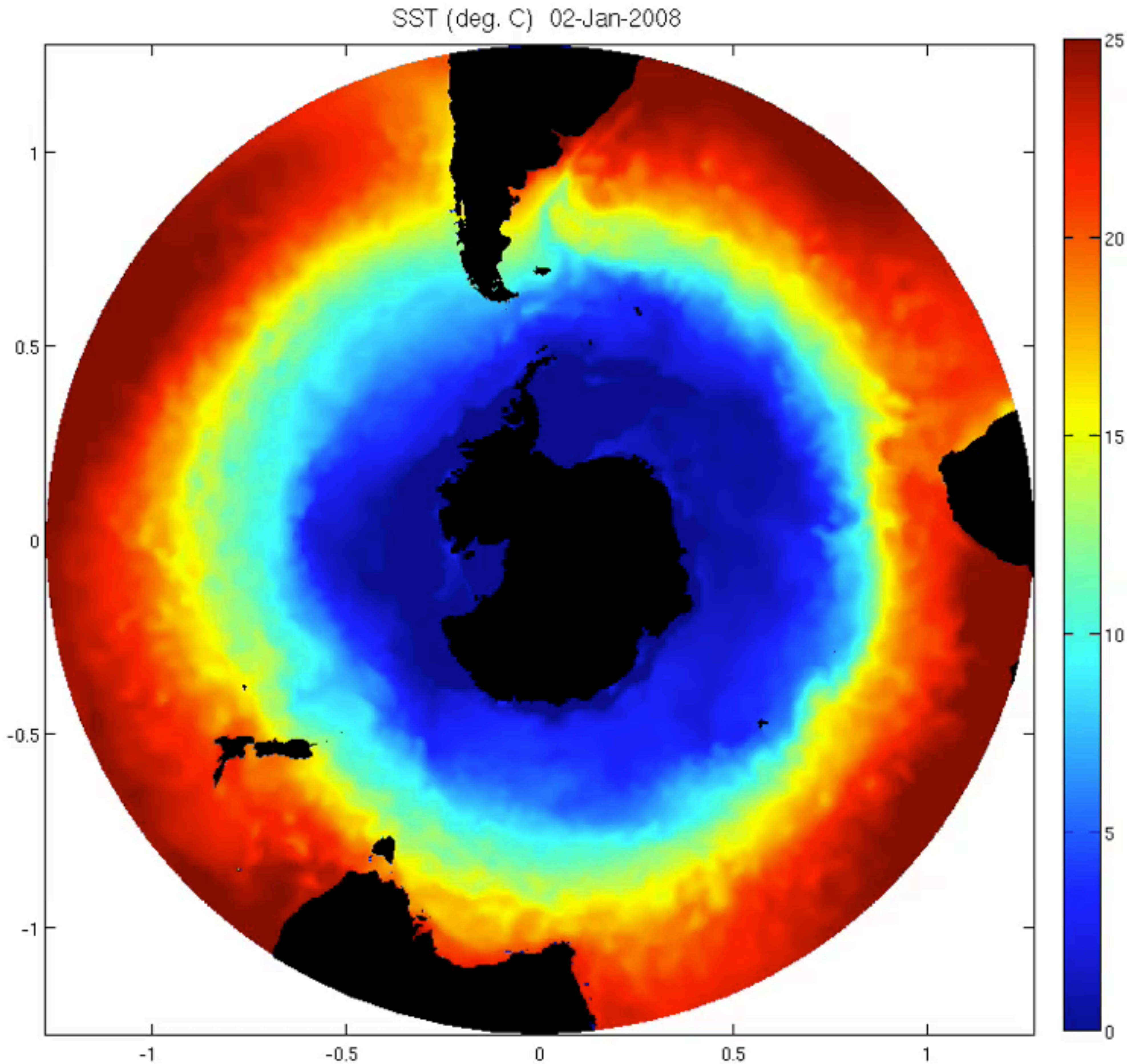
SST (deg. C) 02-Jan-2008
1
0.5
0
-0.5
-1
-1
-0.5
0
0.5
1
25
20
15
10
5
0

Matt Colebrook

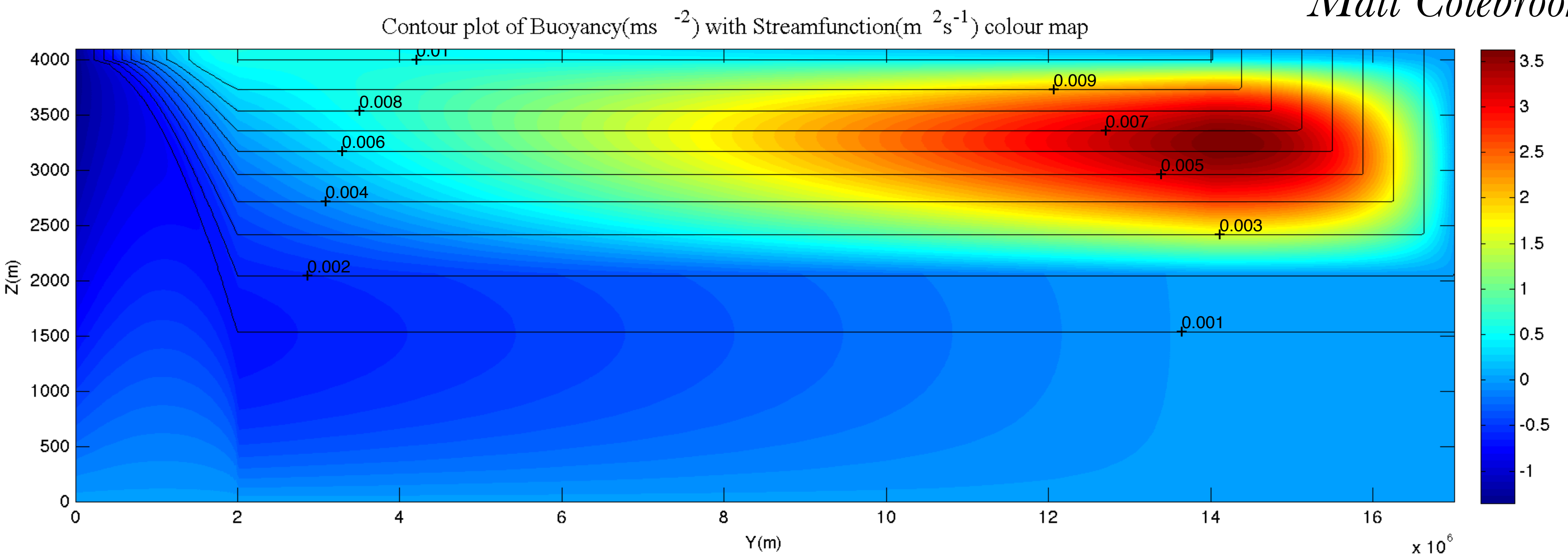

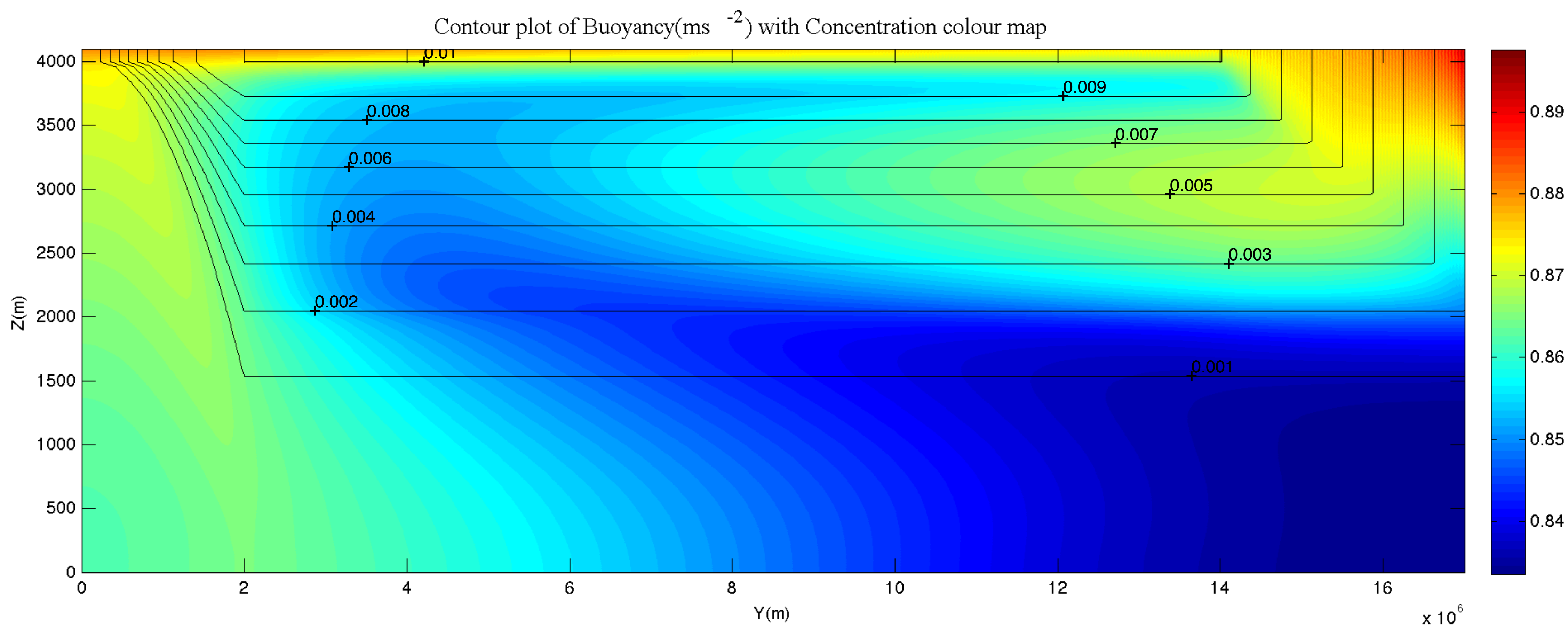

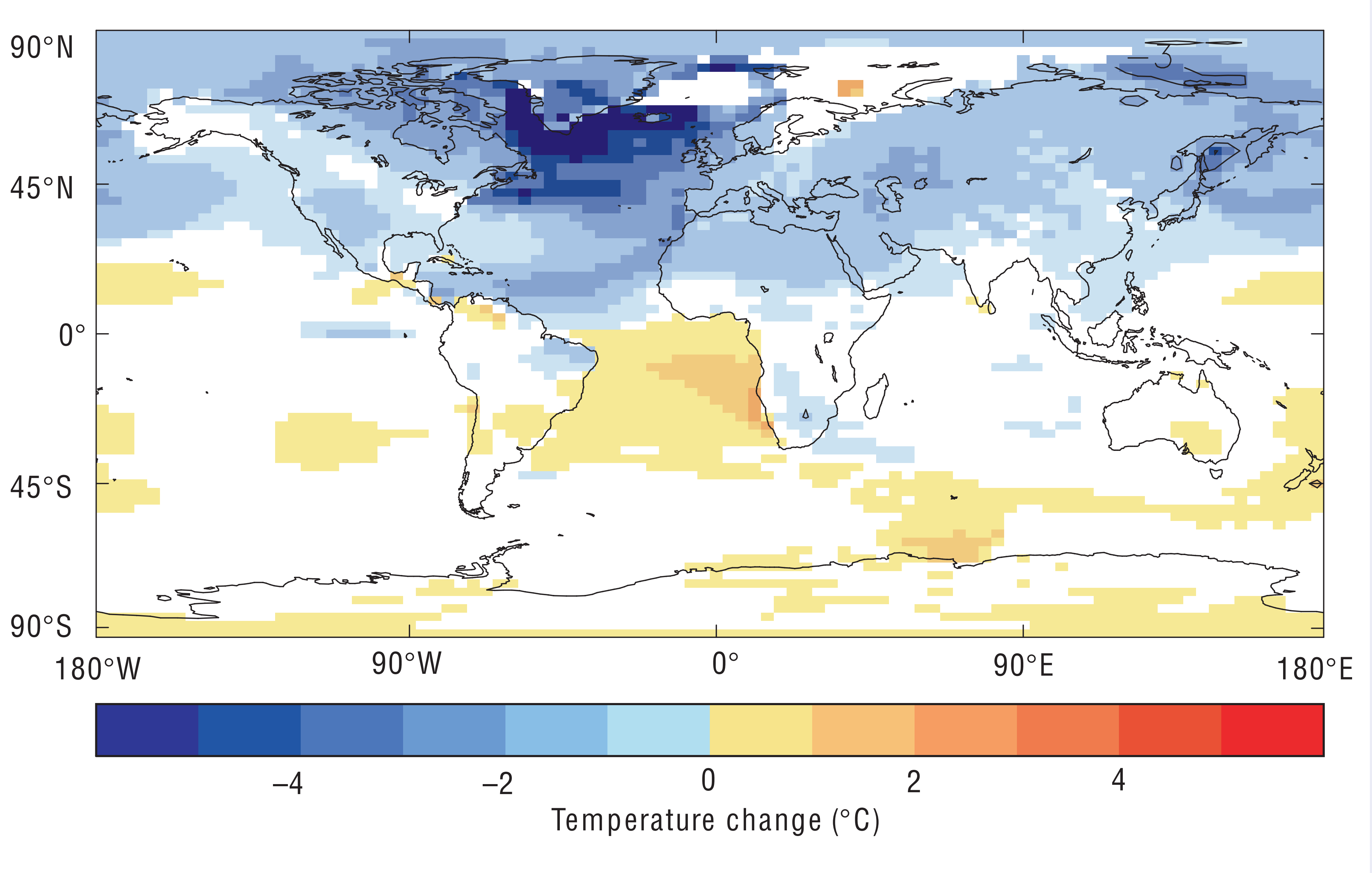

Figure 1 Changes in surface air temperature caused by a shutdown of North Atlantic Deep Water (NADW) formation in a current ocean–atmosphere circulation model. Note the hemispheric see-saw (Northern Hemisphere cools while the Southern Hemisphere warms) and the maximum cooling over the northern Atlantic. In this particular model (HadCM3)[7], the surface cooling resulting from switching off NADW formation is up to 6 °C. It is further to the west compared with most models, which tend to put the maximum cooling near Scandinavia. This probably depends on the exact location of deep-water formation (an aspect not well represented in current coarse-resolution models) and on the sea-ice distribution in the models, as ice-margin shifts act to amplify the cooling. The largest air temperature cooling is thus greater than the largest sea surface temperature (SST) cooling. The latter is typically around 5 °C and roughly corresponds to the observed SST difference between the northern Atlantic and Pacific at a given latitude. In most models, maximum air temperature cooling ranges from 6 °C to 11 °C in annual mean; the effect is generally stronger in winter.

Rahmstorf, Nature, 2002

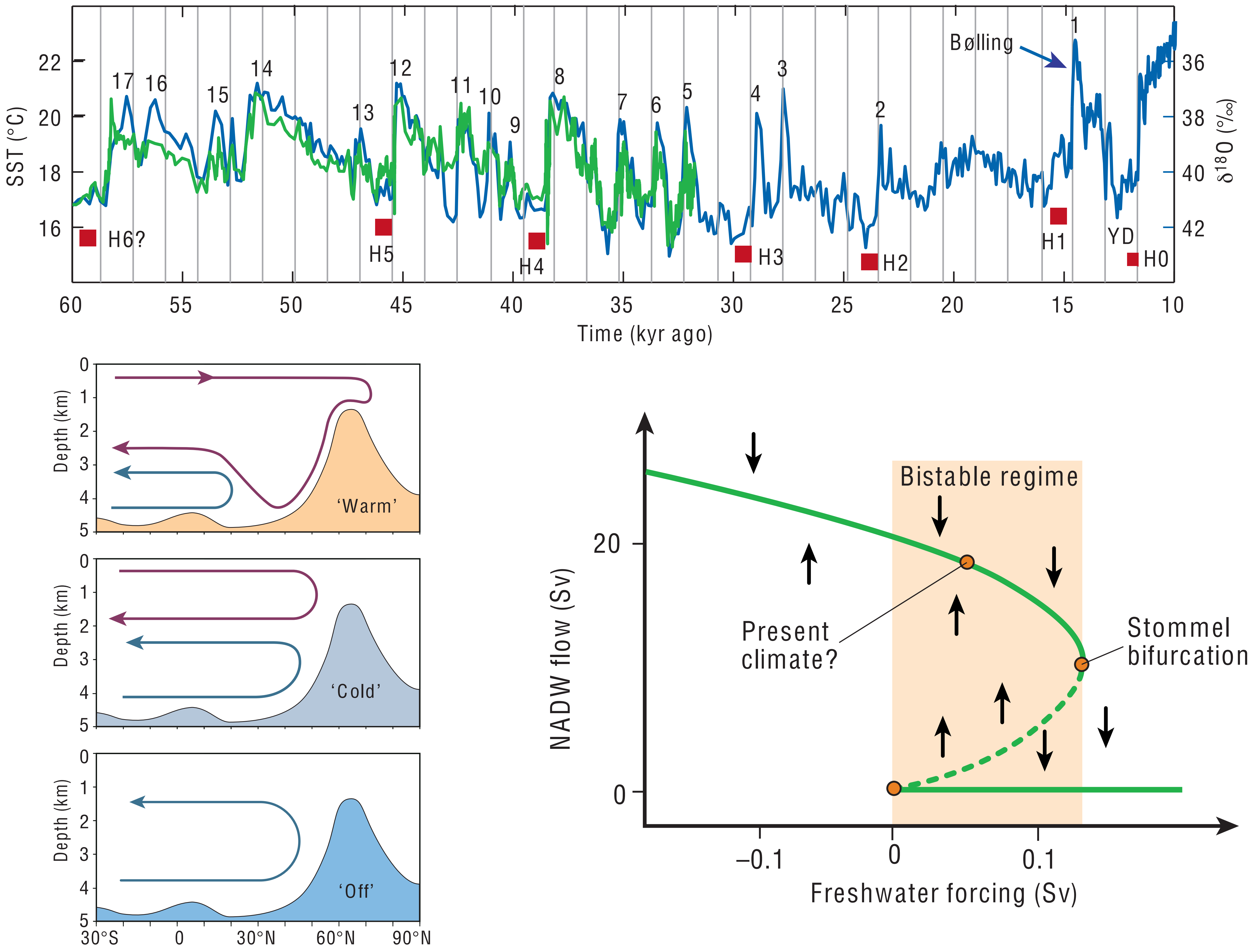
SST (°C)
22
20
18
16
$\delta^{18}O$ (‰)
36
38
40
42
17
16
15
14
13
12
11
10
9
8
7
6
5
4
3
2
1
Bølling
H6?
H5
H4
H3
H2
H1
YD
H0
60
55
50
45
40
35
30
25
20
15
10
Time (kyr ago)
Depth (km)
0
1
2
3
4
5
'Warm'
'Cold'
'Off'
30°S
0
30°N
60°N
90°N
NADW flow (Sv)
20
0
Bistable regime
Present climate?
Stommel bifurcation
−0.1
0
0.1
Freshwater forcing (Sv)